UNITED STATES
NUCLEAR REGULATORY COMMISSION
WASHINGTON, D.C. 20555-0001

January 16, 2024

NOTE TO FILE: Project File: PROJ0734

FROM: Cynthia Barr, Sr. Risk Analyst
Risk and Technical Analysis Branch
Division of Decommissioning, Uranium Recovery
and Waste Programs
Office of Nuclear Material Safety and Safeguards

SUBJECT: SUMMARY AND PRELIMINARY COMMENTS ON DOCUMENTS PROVIDED BY THE UNITED STATES DEPARTMENT OF ENERGY IN SUPPORT OF THE F-TANK FARM AND H-TANK FARM FACILITY PERFORMANCE ASSESSMENTS

The United States Nuclear Regulatory Commission (NRC) and United States Department of Energy (DOE) participated in three meetings in FY2022 to discuss a variety of technical topics related to F-Tank Farm (FTF) and H-Tank Farm (HTF) disposal activities at the Savannah River Site in Aiken, SC. NRC and DOE met in January 2022 (on performance assessment (PA) updates, see ADAMS Accession No. ML22014A069), in March 2022 (on the NRC's HTF Special Analysis technical review report findings, see ADAMS Accession No. ML22094A161) and in April 2022 (on NRC's tank grouting technical review report findings, see ML20296A550). DOE and NRC also participated in one meeting in March 2023 to discuss the status of tank farm PA revisions (see ADAMS Accession No. ML23256A298). During these meetings DOE provided NRC with technical reports developed to support future update to the HTF and FTF PAs.

The purpose of this Note to File is to summarize documents provided by DOE to support updates to DOE's tank farm PAs planned for FY2024 and FY2025. The documents were submitted to NRC to support its monitoring responsibilities under the National Defense Authorization Act for Fiscal Year 2005. Monitoring Factor 6.3 of NRC's SRS Tank Farms Monitoring Plan (see ADAMS Accession No. ML15238A761) is related to PA Maintenance reviews. Because DOE submitted documents on a variety of topics to NRC prior to submittal of the actual updated FTF and HTF PAs, NRC staff are providing preliminary reviews in this note to file on a variety of topics rather than addressing a specific monitoring factor or group of related monitoring factors in separate technical review reports by technical topic. It is important to note that after the updated PAs are submitted, NRC staff will be in a better position to assess the risk-significance of any comments it makes on natural and engineered features of the disposal facilities relied on for performance in this note to file. Therefore, the comments made in this note to file should be reassessed for applicability and risk-significance once the FTF and HTF PAs are submitted to NRC by DOE.

Enclosure: Summaries and Preliminary Review Comments on DOE SRS Tank Farm PA Documents

Summaries and Preliminary Review Comments on DOE SRS Tank Farm PA Documents

The following technical reviewers provided input to this note to file.

George Alexander, Risk Analyst, NRC
Cynthia Barr, Senior Risk Analyst, NRC
Cynthia Dinwiddie, Staff Scientist, Southwest Research Institute®[1]
Osvaldo Pensado, Staff Scientist, Southwest Research Institute®[1]
David Pickett, Senior Program Manager, Center for Nuclear Waste Regulatory Analyses (CNWRA)[2]
Stuart Stothoff, Principal Scientist, CNWRA[2]

[1] The Southwest Research Institute® is a not-for-profit research institute benefiting government, industry, and the public through innovative science and technology, located in San Antonio, Texas 78238.
[2] The Center for Nuclear Waste Regulatory Analyses (CNWRA®) is a federally funded research and development center, which was established in 1987 by the U.S. Nuclear Regulatory Commission. The CNWRA is part of the Chemistry and Chemical Engineering Division of the Southwest Research Institute.

Waste Release Documents

This section discusses three reports expected to provide supporting information for waste release models in upcoming PA revisions. The first report concerns the models of cementitious material degradation processes that affect the evolution of the physical and chemical environment and characteristics of the tank grouts and the radionuclides contained in the tank bottom residue. The second report updates DOE's recommended solubility limits for relevant radioelements in the tank bottoms using prior reports and new modeling. The third report was published just before the other reports and comprises an update to the overall geochemical data package for SRS PAs. Therefore, it also includes DOE's recommendations for geochemical parameters for near- and far-field transport. No attempt was made to reconcile any differing solubility recommendations from the latter two reports because PA recommendations could have changed since those reports were published.

These reports update relevant portions of the following:

- SRNL-STI-2010-00035, Langton, C.A., Chemical Degradation Assessment for the H-Area Tank Farm Concrete Tanks and Fill Grouts, Savannah River Site, Aiken, SC, Rev. 0, January 29, 2010.
- SRNL-STI-2010-00047, Garcia-Diaz, B.L., Life Estimation of High Level Waste Tank Steel for H-Tank Farm Closure Performance Assessment, Savannah River Site Aiken, SC, March 2010.
- SRNL-STI-2012-00404, Denham, M.E. and M.R. Millings, Evolution of Chemical Conditions and Estimated Solubility Controls on Radionuclides in the Residual Waste Layer during Post-Closure Aging of High-Level Waste Tanks, Savannah River Site, Aiken, SC, Rev. 0, August 2012.
- WSRC-STI-2007-00061, Subramanian, K.H., Life Estimation of High Level Waste Tank Steel for F-Tank Farm Closure Performance Assessment, Savannah River Site, Aiken, SC, Rev. 2, June 2008.
- WSRC-STI-2007-00607, Langton, C.A., Chemical Degradation Assessment of Cementitious Materials for the HLW Tank Closure Project, Savannah River Site, Aiken, SC, Rev. 0, September 14, 2007.

SRR-CWDA-2021-00034. Flach, G. "Chemical and Physical Evolution of Tank Closure Cementitious Materials." Revision 0. Aiken, South Carolina: Savannah River Remediation. April 2021.

To support the upcoming HTF and FTF PA revisions, this report provides a summary of DOE's updated cementitious materials degradation approach. For the tank farm tanks, DOE adopted a degradation approach similar to that assumed for saltstone (i.e., degradation based on decalcification), coupled with corrosion of cooling coils in tank fill grout. Several grouts were analyzed, including LP#8-16 reducing tank grout (also referred to as Tank Fill Grout/TFG and Tank Closure Grout/TCG), aggregate-free clean cap grout (as placed into the upper portion of Tank 16H), and slag-free Zero-Bleed CLSM (ZB-FF-8-D) (see C-SPS-G-00096, C-DCF-G-00400, and related reports in Appendix A for more information on ZB-FF-8-D). For concrete vault degradation, DOE also considered corrosion of steel reinforcing bars, the formation of expansive phases, and cracking.[3] Degradation times were calculated for cases that DOE characterized as realistic, compliance, and pessimistic.

[3] For the purpose of concrete vault degradation modeling, DOE assumed the mix was a contemporary mix, B3000-6-0-2-A, because precise compositions are generally unavailable. C-SPS-G-00096 and C-DCF-G-00397 contain additional information on B3000-6-0-2-A mix specifications and properties.

The grout degradation conceptual model for decalcification is based on the advective flow of infiltrating water, calcium leaching at its solubility limit, and the amount of calcium in the cementitious materials. DOE assumes that grout degradation starts after the roof concrete becomes chemically aged (i.e., low dissolved calcium) or physically degraded (i.e., cracked) and that the degradation front advances uniformly from tank top to bottom. DOE calculates the effective hydraulic properties based on an average (e.g., arithmetic, harmonic) of the fractions of the degraded and nondegraded grout and concrete.

This report updates prior studies of steel corrosion rates, K_{sat}, effective diffusion coefficient, and chemical and physical degradation of cementitious materials as functions of time. Chemical grout and concrete evolution analyses were performed with *Geochemist's Workbench*® and *PHREEQC* using custom thermodynamic databases. Physical grout-evolution analyses were performed using simple abstractions solved analytically.

Key NRC Staff Observations:

- NRC staff consider flow through preferential pathways, such as shrinkage gaps, to be the risk-limiting scenario for the Tank Farms.
- The risk significance of DOE's assumed degradation of cementitious materials is unclear. However, if degradation of cementitious materials is risk significant, uncertainties in DOE's approach may be important, including:
    - The potential for additional degradation mechanisms other than decalcification, carbonation, and corrosion;
    - Alternative conceptual models other than that of uniform degradation from tank top to bottom with no preferential flow paths.
    - Concerning averaging of degraded versus intact cementitious material properties into effective hydraulic properties, it is noted that different averaging approaches can significantly affect the assumed hydraulic properties at different times.
- Given that roughly 90 percent of the solids in the cementitious materials tested are amorphous and unidentified or else unreacted minerals, there is uncertainty in the thermodynamic model. Furthermore, as pointed out in SRR-CWDA-2021-00034, *pH* variation is likely to be smooth rather than stepwise, such that *pH* at any one time is not directly predicted by the model. For instance, p. 96 of SRR-CWDA-2021-00034 stated "On average Region III is representative of the 10 > *pH* > 8.3 portion of the gold line." The average of a *pH* range is not relevant when chemical behavior can be markedly different within the range. The next paragraph seems to acknowledge this. NRC will consider this when reviewing how the model results are used in PA.
- In some of the geochemical calculations, the report used PHREEQC to verify GWB results (see Section 2.1). In addition, an analytical calculation was used to verify PHREEQC results in Appendix C. As the report acknowledges, comparing code results is code validation (or benchmarking) rather than model validation. It is not clear the extent to which DOE considered how uncertainties in thermodynamic data and phase selection affect the modeling results and their application in the PA.
- It is unclear how the E_h model results (i.e., transition time to positive E_h) are conservative. The submerged tank sensitivity case in Section 4.1 yields an earlier transition to positive E_h than the base case (compare Figures 4.1-3 and 4.1-24) and was noted to be the only instance in which the base case was less conservative than a sensitivity case.
- It is unclear why using partial hydration leads to accelerated chemical evolution and is therefore conservative. It may be because the initial state (higher Ca/Si, higher *pH*) is further out of equilibrium with the reacting solutions.

SRR-CWDA-2021-00042. Flach, G. "Recommended Solubilities for Tank Closure Performance Assessment Modeling." Revision 0. Aiken, South Carolina: Savannah River Remediation. May 2021.

This report replaces SRNL-STI-2012-00404 by updating the SRS Tank Farms Waste Release Model and refining the representation of equilibrium geochemistry in order to calculate solubility limits for radioelements of interest in the residual waste layer of grouted tanks during future time periods that represent the evolving chemical degradation of reducing tank grout. Equilibrium geochemistry results were generated by coupling *The Geochemist's Workbench*® modeling software with three thermodynamic databases: (i) the Nuclear Energy Agency December 2020 database was used for *Am*, *Np*, *Pu*, *Tc*, *Th*, and *U*; (ii) the Denham and Millings (2012) database (SRNL-STI-2012-00404) was used for *Ba*, *C*, *Eu*, *Ni*, *Sr* and *Y*; (iii) the ThermoChimie v. 10a PHREEQC database (2018) was used for *Co*, *Cm*, *Ra*, *Se*, *Sm*, and *Sn*. This report also considered IEI 2024-002, a 2021 consulting report by Dr. Miles Denham that recommended updated solubilities for Tc, U, Np, Pu, and I. IEI 2024-002 based its recommendations on updated geochemical modeling and comparison to results of laboratory experiments conducted by DOE with Tank 18F and Tank 12H waste.

- DOE assumed that the waste pore solution in non-submerged tanks is equilibrated with and controlled by the chemistry of overlying tank grout. For submerged and partially submerged tanks, DOE assumed that the solubilities may be controlled by the groundwater chemistry or groundwater equilibrated with vault concrete.
- DOE considered two grout-evolution models: a modified version of SRNL-STI-2012-00404 and SRR-CWDA-2021-00034. The modifications to the SRNL-STI-2012-00404 model involved (i) raising the negative Reduced Region II E_h in response to later model and laboratory data and (ii) raising dissolved inorganic carbon values an order of magnitude to more realistically reflect the elevated CO_2 partial pressure in subsurface waters. The SRR-CWDA-2021-00034 model was based on the recommendations in IEI 2024-01, which itself represented an update to the SRNL-STI-2012-00404 model.
- In SRR-CWDA-2021-00042 (Section 4.0), DOE recommended that radioelement solubilities be based on simulated solutions in either the modified SRNL-STI-2012-00404 model or the SRR-CWDA-2021-00034 model, stating that "The underlying grout-evolution models have similar pedigrees and these two sets of solutions and solubilities are equally viable candidates for a PA baseline modeling case."
- For vadose zone tanks based on a modified grout-evolution model in SRNL-STI-2012-00404, DOE's recommended pore-water chemistry for solubility analysis is in Table 2.3-1:

Table 2.3-1: Pore Solutions for Vadose Zone Tanks Based on SRNL-STI-2012-00404.

Attribute (mol/kg)	Reducing Region II	Modified Reducing Region II	Oxidizing Region II	Modified Oxidizing Region II	Oxidizing Region III	Modified Oxidizing Region III
pH	11.1	11.1	11.1	11.1	9.2	9.2
Eh (volts)	-0.47	-0.20	+0.24	+0.24	+0.29	+0.29
DIC	6.7E-07	6.7E-06	6.9E-07	6.9E-06	7.5E-05	7.5E-04
Ca++	4.0E-03	4.0E-03	4.0E-03	4.0E-03	6.6E-05	6.6E-05
SO4--	1.0E-05	1.0E-05	1.0E-05	1.0E-05	1.0E-05	1.0E-05
Na+	1.0E-03	1.0E-03	1.0E-03	1.0E-03	1.0E-03	1.0E-03
Cl-	1.0E-03	1.0E-03	1.0E-03	1.0E-03	1.0E-03	1.0E-03
H4SiO4	–	–	–	–	–	–
Oxalate	4.1E-06	4.1E-06	4.1E-06	4.1E-06	4.4E-05	4.4E-05

Notes: DIC = dissolved inorganic carbon.

- For vadose zone tanks based on the grout-evolution model in SRR-CWDA-2021-00034, DOE's recommended pore-water chemistry for solubility analysis is in Table 2.3-2:

Table 2.3-2: Pore Solutions for Vadose Zone Tanks From SRR-CWDA-2021-00034.

Attribute (mol/kg)	Reducing b	Oxidizing b	Oxidizing c	Oxidizing d	Oxidizing e
pH	11.414	11.4	10.011	8.533	4.3
Eh (volts)	-0.20	+0.21	+0.28	+0.32	+0.37
DIC	8.9E-06	9.6E-06	1.9E-05	8.8E-04	3.4E-04
Ca++	2.3E-03	1.8E-03	1.3E-03	5.5E-04	6.2E-06
SO4--	3.8E-04	4.1E-05	4.1E-05	4.1E-05	4.1E-05
Na+	5.3E-05	5.3E-05	5.3E-05	5.3E-05	5.3E-05
Cl-	5.7E-05	5.7E-05	7.5E-05	5.7E-05	5.7E-05
H4SiO4	2.8E-04	5.2E-04	3.8E-03	1.9E-03	1.9E-03
Oxalate	2.2E-06	2.7E-06	3.4E-06	6.3E-06	–

Notes: DIC = dissolved inorganic carbon.

- For submerged tanks, DOE's recommended pore-water chemistry for solubility analysis is in Table 2.3-3:

Table 2.3-3: Pore Solutions for Submerged CZ Tanks.

	SRR-CWDA-2021-00034		SRNL-STI-2012-00404
Attribute (mol/kg)	Oxidizing GW+Calcite	Oxidizing GW	Condition A (GW)
pH	8.441	5.4	5.4
Eh (volts)	+0.37	+0.37	+0.37
DIC	7.5E-04	3.8E-04	9.8E-05
Ca++	4.5E-04	7.5E-05	6.2E-05
SO4--	2.4E-05	2.4E-05	6.3E-06
Na+	4.6E-05	4.6E-05	4.4E-05
Cl-	1.6E-04	1.6E-04	8.5E-05
H4SiO4	7.7E-05	7.7E-05	–
Oxalate	7.5E-06	–	4.2E-05

Notes: DIC = dissolved inorganic carbon.

- The following tables compare the solubilities of key radionuclides assumed in the F- and H-Tank Farm PAs with the revised modeled solubilities with the highest experimentally observed values from laboratory studies with actual waste.

	Neptunium						
	RRII	ORII	ORIII				
FTF PA	2E-09	2E-05	1E-04				
HTF PA	1E-09	3E-07	2E-06				
SRR-CWDA-2021-00042	Modified RRII	Modified ORII	Modified ORIII				
	1.0E-09	5.8E-09	6.0E-06				
SRR-CWDA-2021-00042	Reducing b	Oxidizing b	Oxidizing c	Oxidizing d	Oxidizing e	Oxidizing GW + Calcite	Oxidizing GW
	1.00E-09	3.00E-09	1.00E-06	7.40E-06	2.30E-05	4.30E-05	2.30E-05
Highest Experimentally Obseved Value	RRII	ORII	ORIII	ORII and ORIII Wash			
	2.90E-08	2.40E-09	7.90E-09	2.90E-08			
Factor of Modeled Optimism	29	0	0	5			

	Plutonium						
	RRII	ORII	ORIII				
FTF PA	4E-12	4E-14	6E-05				
HTF PA	3E-11	3E-11	3E-11				
SRR-CWDA-2021-00042	Modified RRII	Modified ORII	Modified ORIII				
	1.5E-11	1.5E-11	1.5E-11				
SRR-CWDA-2021-00042	Reducing b	Oxidizing b	Oxidizing c	Oxidizing d	Oxidizing e	Oxidizing GW + Calcite	Oxidizing GW
	1.5E-11	1.5E-11	1.5E-11	1.5E-11	1.30E-08	1.5E-11	1.10E-10
Highest Experimentally Obseved Value	RRII	ORII	ORIII	ORII and ORIII Wash			
	4.50E-09	8.50E-09	2.00E-08	3.00E-07			
Factor of Modeled Optimism	300	567	1333	20000			

(Note that steady-state conditions were not achieved for plutonium, therefore the values could be higher than observed.)

	Technetium						
	RRII	ORII	ORIII				
FTF PA	3E-11	3E-13	No Solubility Control				
HTF PA	1E-14	1E-13	2E-15				
SRR-CWDA-2021-00042	Modified RRII	Modified ORII	Modified ORIII				
	1.4E-04	No Solubility Control	No Solubility Control				
SRR-CWDA-2021-00042	Reducing b	Oxidizing b	Oxidizing c	Oxidizing d	Oxidizing e	Oxidizing GW + Calcite	Oxidizing GW
	2.50E-03	No Solubility Control	No Solubility Control	No Solubility Control	No Solubility Control	No Solubility Control	No Solubility Control
Highest Experimentally Obseved Value	RRII	ORII	ORIII	ORII and ORIII Wash			
	1.10E-08	1.30E-08	1.20E-08	1.00E-08			
Factor of Modeled Optimism	0	0	0	0			

	Uranium						
	RRII	ORII	ORIII				
FTF PA	2E-09	2E-11	3E-05				
HTF PA	5E-09	5E-05	4E-06				
SRR-CWDA-2021-00042	Modified RRII	Modified ORII	Modified ORIII				
	2.7E-06	2.7E-06	4.7E-05				
SRR-CWDA-2021-00042	Reducing b	Oxidizing b	Oxidizing c	Oxidizing d	Oxidizing e	Oxidizing GW + Calcite	Oxidizing GW
	5.10E-06	5.00E-06	6.10E-07	1.30E-04	2.60E-03	9.00E-05	9.60E-05
Highest Experimentally Obseved Value	RRII	ORII	ORIII	ORII and ORIII Wash			
	6.50E-04	4.20E-05	4.20E-04	4.60E-03			
Factor of Modeled Optimism	241	16	9	1704			

Key Findings and Recommendations:

- The disparity between the modeled solubilities and experimentally observed dissolved concentrations of Pu and U suggest that either (i) the assumed phases controlling dissolved species are incorrect or (ii) the environmental conditions for the radionuclides that were studied in the development of the database differed from those during the laboratory studies of tank farm waste. (See, for example, the discussion in ML21026A012.)
- Although DOE does not project the "Oxidizing d" and "Oxidizing e" conditions to occur until after 4000 and 6000 pore volumes[4], respectively, the modeled solubility of Pu in condition "Oxidizing e" is in the range of the highest experimentally observed values. For U, its modeled solubility in conditions "Oxidizing d" and "Oxidizing e" is in the range of the highest experimentally observed values.
- It is unclear what chemical conditions and solubility values DOE will assume in future PAs.
- However, if DOE selects the chemical conditions and solubility values recommended in SRR-CWDA-2021-00042, contaminant release could be underestimated by orders of magnitude, especially for Pu and U.
- NRC will continue to monitor the assumed chemical conditions and solubility values for key radionuclides and the technical bases for these assumptions. For example, NRC staff generally regard laboratory studies of actual waste to be more credible than model results because laboratory studies can provide directly relevant information if the conditions are representative of the field conditions. Geochemical modeling studies have several limitations that lead to uncertainty in model results:
    - There can be significant differences in the phases of the radionuclides that are in the actual waste versus the radionuclides studied in the development of geochemical databases used in the geochemical modeling studies.
    - There can be significant differences in the environmental conditions that will occur in the field versus the conditions applied to experiments conducted to develop geochemical databases.
    - Geochemical modeling assumes equilibrium conditions that may not apply.
    - DOE assumed that groundwater was conditioned under most assumed conditions except for the "Oxidizing e" and the "Oxidizing GW" conditions. DOE assumed approximately 1 order of magnitude reduction in solubility for Pu when submerged tanks are conditioned by vault concrete. It is unclear how long DOE assumes this condition will persist and how long this condition will exist in the field.

Follow-up Action Items and Questions:

1. Many dissolved species were eliminated to simplify *The Geochemist's Workbench*® models. Could DOE clarify how it ensured that these omissions would not affect calculated solubilities? For instance, Al and K can affect silicate mineral solubilities, which can affect dissolved silica and, therefore, uranophane solubility.
2. Could DOE clarify if saturation indices for other solids for a given radioelement were checked for supersaturation? Did DOE have to suppress any phases and, if so, were those suppressions justified?
3. DOE should confirm that of the more important radioelements, only U solubilities were updated based on new experimental data.

[4] Without the PA, it is not clear when DOE projects 4000 pore volumes will have flushed through the grout.

4. The results present modeled solubilities. Will DOE consider any other data from waste-release experiments or other sources for the updated PA? For instance, Pu solubilities changed little from the 2012 report (i.e., SRNL-STI-2012-00404). All values are approximately 1×10^{-11} M except at $pH < 6$, where the Pu solubility does not exceed 1×10^{-8} M.

SRNL-STI-2021-00017, Rev. 0. Geochemical Data Package for Performance Assessment Calculations Related to the Savannah River Site. February 2021.

This report presents an updated compilation of distribution coefficient (K_d), apparent solubility (k_s), and cementitious leachate impact factor values for performance assessments (PAs) and related analyses of radioactive waste disposal and waste tank closure at the Savannah River Site (SRS). The previous data package was published in 2016 (D. Kaplan, "Geochemical Data Package for Performance Assessment Calculations Related to the Savannah River Site," SRNL-STI-2009-00473. Rev. 1). Because SRNL-STI-2021-00017 was published nearly three years ago, and subsequent analyses of these parameters have likely been performed, a detailed technical review of selected values was not attempted—nor was an attempt made to contrast the apparent solubilities with the values recommended a few months later in SRR-CWDA-2021-00042. An opportunity to perform such a focused, risk-informed review is expected soon when the H-Area Tank Farm PA is published. The current review involves more general comments about the approaches and results described in the report. It is noted that the report effectively describes the factors affecting radionuclide release and transport in the various environments at SRS. NRC reviews of this type of data focus on application to the Saltstone Disposal Facility and Closed Liquid Waste Tanks (described in Sections 5.6 and 5.7, respectively). The particular parameters and approaches adopted in future PAs may render some of these comments inapplicable.

Key Observations

Use of more data. Since the 2016 data package, DOE investigators have accumulated and evaluated a great deal of new data, both from the literature and from site-specific studies. It is therefore surprising that, according to the table on page 12 (SRNL-STI-2021-00017), very few changes have been made to recommended K_d values that could have a significant impact on PA results. There were apparently no or minimal changes to potentially important radioelements Tc and I and only one minor change to Pu. For cementitious conditions, for which the report states a wealth of new information has become available, K_d values were changed for only two elements (As and Sb)—and those changes were not large. No potentially significant changes to k_s values were noted.

The paired K_d and k_s concept. The report introduces more “pairs” of K_d *and* k_s values for elements in cementitious environments. The concept seems necessary only for certain cases in which the same redox condition is not used for both values (Section 6.1). The need for these different pairs for redox-insensitive elements Ba, Sr, and Ra for reoxidized systems is described in Table 19. The report recommends developing paired values for other elements, including redox-sensitive U and Pu, and NRC will evaluate any such changes in the H-Area Tank Farm PA.

Use of more mechanistic models. NRC agrees that developing more mechanistic reactive transport models—that, for example, incorporate surface complexation—should be a high priority. Such an approach would be particularly useful to better modeling the behavior of more geochemically complex radioelements such as I and Pu, the transport of which may be underestimated by simple K_d approaches. NRC agrees also with the other recommendations for

additional studies (Section 7) and will look for any advances that were incorporated into parameters for the H-Area Tank Farm PA.

Probability distributions. The change to employing log-normal distributions for K_d *and* k_s in stochastic models is well-reasoned. However, the bases for the particular uncertainty bounds proposed (Section 4.8) are not always clear. For example, a bullet on page 47 states that "The width of 95% confidence interval for the estimated mean K_d was twice the mean in the Aquifer Zone (Sandy Sediment Environment)…" As written, this implies a linear range from zero to twice the mean, even though it was previously stated that a log-normal distribution is used. In addition, the relationships between the multipliers used in Equations 11 to 14 and the description of the ranges in the preceding text were not explained.

The uncertainty bounds for K_d values are relatively narrow; the range for a sandy sediment is from one-half to twice the mean value, and the range is even narrower for clayey sediment (Equations 11 to 14). Although the quantities were based on K_d measurements on ten elements on multiple sediment samples, a basis was not provided in this report for why those ranges would be applicable for PA in a system in which there is uncertainty in the geochemical conditions. Consider Stage III, which, based on discussions in the report, could experience *pH* values of between 11 and 8 as CSH gel dissolves. K_d for some elements could vary considerably over that *pH* range, a variation that a narrow uncertainty range around a single mean value would not reflect. Furthermore, a basis was not provided for why data from these ten elements would collectively reflect the uncertainty in K_d for potentially significant radioelements with more complex geochemical behavior (e.g., I and Pu).

Finally, a basis was not provided for the assumption of a two-order-of-magnitude uncertainty range for k_s values.

Steel Liner Performance

SRNL-STI-2021-00187. Wiersma, B.J. “Corrosion of Steel During Long-Term Exposure to Evolving Cementitious Environments.” Revision 0. Aiken, South Carolina: Savannah River Remediation. April 2021.

DOE developed a revised corrosion model to predict steel-liner performance that attempted to better couple cementitious material performance and degradation modeling with steel liner performance/corrosion modeling. Four different cases were considered: (i) realistic case, (ii) compliance case, (iii) pessimistic case, and (iv) fast-flow path case. Failure times for steel liner components (floor, wall, and roof) for each tank type for tanks located in the vadose zone and for the portion of any steel liners that are located below the water table surface are provided below in Tables 9.1 through 9.2. Failure times for cooling coils are also provided in the report.

Modeling results for the realistic, compliance, and pessimistic cases include a limiting damage or degradation time following: (i) arrival time of relatively low *pH* depassivation front due to carbonation, and (ii) the environmental exposure and loss of passivation due to anoxic rebar corrosion. For four of the six cases, degradation of the rebar due to anoxic corrosion results in the limiting time. Carbonation is the limiting time only for the compliance and pessimistic cases for the vadose zone due to higher gas phase diffusion coefficients and shorter damage front lag. The damage times for the saturated zone range from as low as 2,100 yrs for Type IV tanks (pessimistic) to as long as 23,000 yrs for Type II tanks (realistic and compliance). For the vadose zone, damage times are as low as 75 yrs for Type IV tanks (pessimistic) to 23,000 yrs for Type II tanks (realistic).

In the realistic case, DOE assumes no gaps exists between the steel liner and grout and no cold joints exist in the vault. In the compliance case, DOE considers a gap at the tank grout/steel liner interface on the roof, and cold joints through the vault. For the pessimistic case, DOE includes gaps between the tank grout and steel liner at the roof, and walls; and cold joints in the vault, as well as structure cracks on the floor leading to higher diffusion coefficients. However, the pessimistic case does not include fast-flow paths and humid air until after the concrete degrades. General corrosion rates (e.g., 1 μm/yr or 0.04 mil/yr) are assumed for initial conditions for most of the scenarios except for the pessimistic case, which assumes higher, initial indoor air corrosion rates.

DOE also considered a steel-corrosion scenario with fast-flow paths where there is a gap between the steel liner and the concrete/grout filled with groundwater or humid air. The scenario was not run for design or compliance purposes, or even characterized by DOE as being plausible, but rather to show the importance of cementitious material on steel liner failure times. In the fast-flow case, DOE assumed that humid air was present in the gaps, if in the vadose zone, or the steel liners were in contact with groundwater, if in the saturated zone. Key assumptions for the tanks in the vadose zone in contact with humid air include the following:

- Critical humidity is always maintained.
- There are no contaminants of consequence on the tank surface.
- Oxygen is always available.
- The humid air corrosion rate was based on the corrosion rate of A516 Grade 55 coupons developed for the Yucca Mountain project.

Section 3.6 of SRNL-STI-2021-00187 discusses results of corrosion rate experiments conducted with Yucca Mountain project carbon steel corrosion coupons. The coupons were exposed to vapor space above a simulated dilute water for 1 yr at 60 and 90 °C [140 and 194 °F]. The data for the test indicate a higher corrosion rate compared to that from aqueous

exposure potentially due to carbon dioxide evolution from carbonate in solution. Additionally, the corrosion rates were higher on average during the 6-mo versus 12-mo tests and the corrosion rates were higher at higher temperatures. DOE averaged the corrosion rates for the 6-mo and 12-mo tests and the 60 °C [140 °F] and 90 °C [194 °F] results and calculated an average corrosion rate of 51.5 µm/yr [2 mil/yr]. DOE then determined the failure time by dividing the thickness of the steel by twice (2×) the corrosion rate, to account for corrosion on the inside and outside of the tanks.

For tanks in contact with groundwater, the following assumptions were applied:

- Vault concrete is completely degraded, allowing groundwater to flow freely to the steel.
- Tank components are located at or below the water table.

Data from the National Bureau of Standards (NBS) was used to estimate corrosion rates of steel in groundwater. The NBS soil type with the highest moisture content and a *pH* similar to SRS soils was muck from New Orleans, Louisiana. The weight-loss and maximum penetration data for open-hearth steel plate was used to calculate the corrosion rate and maximum penetration rate for localized corrosion. The long-term corrosion rate was estimated to be approximately 2 mil/yr. A pitting model was used to estimate the time to breach 25 percent of the steel section being evaluated (i.e., roof, wall, floor) assuming a maximum pit depth, corrosion allowance and number of penetrating pits per container.

Evaluation of Corrosion Rates

NRC considers the realistic and compliance cases potentially overly optimistic because they do not consider any mechanisms that could lead to higher than anoxic (or very low general) corrosion rates for long periods of time. While the pessimistic case relies on an indoor air scenario with higher corrosion rates compared to the passive general corrosion rate, the service conditions are weakly linked to the expected tank conditions. The fast-flow case is run to provide information on the importance of the cementitious materials surrounding the steel components; however, the scenario assumptions regarding degraded cementitious material performance are characterized as being bounding. Still, the corrosion rates simulated in the fast-flow case may be more reflective of expected conditions based on existing information (e.g., grout tests conducted at the CNWRA which showed annular gaps around internal tank fixtures, between grout pours or lifts, and along the tank wall) and a lack of data demonstrating shrinkage will not occur. Therefore, NRC staff focused its review comments on key assumptions made in the fast-flow case.

The assumption of critical humidity and availability of oxygen appear to be reasonable given the presence of the tanks near or within the water table, and high saturated oxygen concentrations in the aquifer (or sufficient oxygen availability in the vadose zone). Also, two-sided corrosion may be conservative depending on the condition of the vault concrete.

The assumption of no contaminants of consequence on the surface of the liner may be optimistic and the impact of steel liner contamination on corrosion rates is unclear. Multiple FTF and HTF tanks have been documented as having salt nodules on the liners (see summary of Annual Radioactive Waste Tank Inspection Program, SRR-STI-2019-00119 in Appendix A). However, the composition of the salt nodules and therefore their risk significance is not clear in those reports. Additionally, observations of groundwater in-leakage into tanks may indicate that steel liner integrity has been compromised in a short period relative to the performance period.

The averaging of the tests conducted with Yucca Mountain project coupons for estimating corrosion rates for humid air appears to be conservative because the corrosion rates slowed between the 6-mo and 12-mo tests and the temperatures are relatively high compared to typical

subsurface temperatures, although the temperature may be more representative during early curing periods.

It is important to note that the type of carbon steel used in the Yucca Mountain project tests (A516, Grade 55) differs from steel used in the tank farms (e.g., Type I [ASTM A285-50T, Grade B Steel] and Type II [A285 Grade B] tanks, primary liner of the Type IIIA[5] tanks [ASTM Type A537], and Type IV steel liners [A285 for FTF Tanks 17-20; and A212 for HTF Tanks 21 through 24]), in addition to potential differences in service conditions, described above. Therefore, it is unclear how representative the Yucca Mountain Project corrosion rate estimates would be for the FTF and HTF tank conditions initially and during the closure period.

Table 9-1. Summary of Failure Times (years) for the Saturated Zone for the Scenario Cases by Tank Type

	Saturated Zone			
Tank Type	Realistic Case (years)	Compliance Case (years)	Pessimistic Case (years)	Fast Flow Path Case (years)
I	3929-6250	3929-6250	625-3941	13-65
II	6250-10938	6250-10938	704-6250	14-65
III/IIIA	4688-10938	4688-10938	625-6250	13-59
IV	2495-5469	2495-5469	852-2477	20-42

Table 9-2. Summary of Failure Times (years) for the Vadose Zone for the Scenario Cases by Tank Type

	Vadose Zone			
Tank Type	Realistic Case (years)	Compliance Case (years)	Pessimistic Case (years)	Fast Flow Path Case (years)
I	4008-6250	2960-6250	625-850	123-502
II	6250-10938	4280-8719	704-1136	123-502
III/IIIA	4688-10938	3860-7751	625-1078	92-441
IV	2569-5469	1082-1127	263-367	181-226

Key Findings and Recommendations:

[5] Type III tanks are constructed of A516 carbon steel.

- While DOE's analysis reflects improvement in the coupling of cementitious material and steel-liner degradation, lack of consideration of an important mechanism (i.e., rebar corrosion due to carbonation leading to accelerated concrete degradation and eventually causing depassivation of the steel liner) does not appear to be addressed in SRNL-STI-2021-00187. NRC staff note that Chapter 7 of SRR-CWDA-2021-00034 may explain the lack of consideration of this mechanism. SRR-CWDA-2021-00034 presents a conceptual model for rebar corrosion due to carbonation with a concrete damage zone that trails the carbonation front. The report concludes that the concrete damage zone would take tens of thousands of years to reach the steel liner. While the analysis may be valid, it appears untested and unvalidated. Without empirical support, rebar corrosion causing concrete cracking and spalling (due to the expanded volume of iron corrosion products) should not be ruled out as a mechanism for enhanced transport of low-pH porewater with eventual depassivation of the steel liner and potentially faster liner failure. The model in SRR-CWDA-2021-00034 contains important uncertainties that have not been fully explored, such as the location of the concrete damage zone with respect to the carbonation front and uncertainty in transport properties of the degraded concrete. Therefore, some previous technical issues raised in NRC staff's FTF and HTF technical evaluation reports (TERs; ML112371751 and ML14094A514) appear to remain pertinent. In the HTF TER, NRC staff wrote the following:

  > *Penetration of carbon dioxide by diffusion is linked to carbonation of the concrete and depassivation of the rebar. Corrosion of the rebar leads to formation of corrosion products. The expansion in volume of the rebar due to the formation of corrosion products can crack reinforced concrete and cause spalling. DOE postulates that failure of the reinforced concrete vault occurs when the carbonation front penetrates 50 percent of the wall thickness. As discussed in the FTF TER (see Section 4.2.9.1; Camper, 2011 [ML112371751]), the technical basis for this failure criterion is not clear, especially since failure criteria in technical literature are more commonly defined on the basis of the thickness of the rebar cover (Parrot, 1990; Andrade et al., 1993; Molina et al., 1993; Neville, 1996). Gradual cracking of the reinforced concrete vault may cause feedback on the rate of transport of carbon dioxide causing a local lowering of the porewater pH, activation of the rebar, and eventually activation of the liner.*

- DOE's assumptions related to diffusion coefficients in the various cases are also unclear. For example, the compliance case considers gaps and cold joints for initial conditions, but the impact of these assumptions is unclear.
- DOE assumes that 25 percent of the tank must be breached via pitting corrosion prior to failure of the tank. The basis for this failure extent requires additional support.
- Tanks 12, 14, 15, and 16 were initially assumed to be failed in the HTF PA due to the number or location of corrosion sites. DOE should clarify whether any tanks are assumed to be initially failed in the updated analysis.
- The primary and secondary liners are assumed to fail at the same time in the HTF PA. This assumption appears to no longer be the case in the updated steel liner failure analysis. Please clarify the differences in key assumptions in the previous PA and the updated PA.
- If DOE relies on this study to demonstrate that the tanks will not leak for extended periods of time, NRC staff should document concerns with observations of leakage in the following tanks (SRMC-STI-2022-00154 and SRMC-STI-2023-00011)[6]:

[6] Review of annual tank inspection reports are summarized in Appendix A.

- Tank 1 (Type I)
- Tank 4 (Type I)
- Tank 9 (Type I)
- Tank 10 (Type I)
- Tank 11 (Type I)
- Tank 13 (Type II)
- Tank 14 (Type II)
- Tank 15 (Type II)

- DOE's analysis indicates that corrosion will not lead to leakage for thousands of years in their realistic and compliance cases. NRC staff acknowledge that grouting the tanks and annuli will reduce the potential for corrosion. However, grouting is unlikely to arrest corrosion that has already been documented, given the likely occurrence of shrinkage gaps. The following tanks have documented corrosion:
    - Tank 23 (Type IV)
    - Tank 30 (Type III): incipient pitting
    - Tank 31 (Type III): incipient pitting
    - Tanks 30, 31, and 32 (Type III): authors commented that the pits are consistent with pre-service pitting with no evidence of active corrosion or growth
    - Tank 47 (Type IIIA): 1 pit on lower plate of primary
- Has DOE considered cracking of welds due to various mechanisms (e.g., weld residual stress, stress corrosion cracking), which was observed in Tank 15?
- Unless DOE can demonstrate that shrinkage gaps will not occur between the grout and the steel liner, the presence of fast-flow paths should be considered in the base case/compliance case.
- The technical bases for the realistic case, compliance case, and pessimistic case are irrelevant unless DOE can demonstrate that shrinkage gaps will not occur. Shrinkage gaps represent a common cause failure point for steel-liner performance and groundwater conditioning by tank fill grout. In other words, shrinkage gaps could significantly decrease overall barrier performance of the grouted tank systems.

Engineered Cover and Erosion Documents

SRR-CWDA-2021-00043. Brush, B. “Erosion Analysis for the F-Area Tank Farm and H-Area Tank Farm Facilities.” Revision 0. Aiken, South Carolina: Savannah River Remediation. April 2021.

This report considers an erosion analysis for the F-Area and H-Area Tank Farm Closure Caps, following methodology developed for Z Area in SRR-CWDA-2021-00036. The erosion analysis considers (i) sheet and rill erosion and (ii) the potential for gully erosion. The erosion analysis is limited to the relatively flat-lying top of the cap and, unlike SRR-CWDA-2021-00036, does not consider the cap side slopes (where the driving forces for erosion are stronger). SRR-CWDA-2012-0043 included a summary of global slope-stability analyses provided by K-CLC-G-00111 (in which large-scale movements from static and seismic loading conditions were analyzed without considering stability of the interface between geosynthetics and engineered soil layers).

The note to file addresses only the erosion analyses in SRR-CWDA-2021-00043. A complete erosion analysis would also consider the side slopes, the transition from flat-lying cap to side slope, and channels between caps.

NRC staff reviewed the analyses in SRR-CWDA-2021-00036 and K-CLC-G-00111 as part of two Technical Review reports [Technical Review: Site Stability at the U.S. Department of Energy Savannah River Site Saltstone Disposal Facility (ML23017A114) and Technical Review: Percolation Through and Potential Erosion near the Closure Cap of the U.S. Department of Energy 2020 Performance Assessment for the Saltstone Disposal Facility at the Savannah River Site (ML23017A083)], both dated April 2023. The 2023 Site Stability Technical Review considered analyses specific to the SDS Closure Cap; the erosion analysis in the other technical review focused on areas downslope of the SDS Closure Cap in Z-Area.

- NRC staff determined that the DOE analysis of gully erosion did not allow the NRC staff to make a determination about site stability because (i) the probable maximum precipitation (PMP) was inconsistent with NRC guidance that suggested use of 246 mm/hr [9.7 in/hr] for a 15-min PMP instead of 69 mm/hr [2.7 in/hr] as used in SRR-CWDA-2021-00036; (ii) the PMP did not factor in climate change, and (iii) several parameters may be affected by elevated water levels above the geomembrane (GMB) layer caused by degradation of the Upper Lateral Drainage Layer (ULDL).
- NRC staff determined that the Revised Universal Soil Loss Equation (RUSLE) approach for sheet and rill erosion was acceptable but is concerned that saturated conditions developing above the GMB layer may rise close enough to the surface to adversely affect several RUSLE parameters.
- NRC staff were unable to make a determination about site stability from K-CLC-G-00111. The stability analyses were incomplete because the closure cap design and implementation plans have not been finalized.

Comments in the NRC Technical Reviews are directly applicable to SRR-CWDA-2021-00043 because of similarity in designs for the FTF, HTF, and SDF Closure Caps. The following provides supplemental discussion of the erosion components. Site stability is not discussed because SRR-CWDA-2021-00043 provides no additional analysis of site stability.

Sheet and Rill Erosion

The erosion analysis for sheet and rill flow is based on the RUSLE from the USDA’s Agricultural Handbook: Predicting Soil Erosion by Water: A Guide to Conservation Planning with the RUSLE

(USDA-HDBK-703). Sheet and rill erosion represents widespread erosion before the water reaches a drainage channel.

The RUSLE approach uses a set of erosion measurements performed on standard plots with reference length, slope, precipitation, soil type, soil permeability, and cover. The standard measurements are scaled by site-specific factors. The RUSLE formula is:

$$A = R\,K\,L\,S\,C\,P$$

where A is the spatial and temporal average soil loss per unit area, R is a rainfall-runoff-erosivity factor plus a snowmelt-runoff factor for a specified recurrence interval, K is a soil-erodibility factor for the specified soil on a standard plot, L is a slope-length factor, S is a slope-steepness factor, C is a cover-management factor, and P is an erosion-control factor. A has units of mass per area per time (e.g., ton/acre/year). The rate of soil removal is converted to units of length per year by dividing A by the bulk soil density. All other parameters besides R and K are dimensionless. The R parameter is expressed for a given recurrence interval matching the time unit of A; the units of the K parameter match the mass and area units of A after canceling the other units of the R parameter.

R is obtained using the largest annualized value from three published sources [250, 300, and 350 hundreds of (ft ton in)/(acre hr yr), respectively]. The K value is assumed to be the largest from estimated values for selected site soils, which have a range of 0.02 to 0.28 tons/acre per unit of R. L and S were combined and determined by interpolation in Table 4-1 from USDA-HDBK-703, using the nominal cap slope and the maximum cap slope lengths. C is based on an assumed cover succession of (i) grass until 140 yrs after closure (C is 0.15), (ii) transitional woodland shrub until 460 yrs after closure (C is 0.05), and (iii) pine forest, thereafter (C is 0.003), using the upper bound of category-specific cover values developed from remote sensing in the European Union. P is given a value of 1 based on taking no credit for deployment of erosion-control practices. The change in C results in greatly reduced sheet and rill erosion once a pine forest is established.

The RUSLE parameters and calculations are consistent with SRR-CWDA-2021-00036. NRC staff confirmed that the RUSLE calculations were applied consistently with the USDA-HDBK-703 equations for average soil loss for the three assumed cover conditions. Note that SRR-CWDA-2021-00043 does not consider the spatial distribution of parameters and erosion across the cap.

The following discussion is supplemental to the 2023 NRC Technical Reviews, based on checks of the RUSLE calculations that considered uncertainty and variability for the input parameters.

- The USDA-HDBK-703 erosion rate increases with distance from the cap ridge, with the erosion rate at the end of the slope ~2x higher than the rate at the top of the slope, and values for the base of the slope are ~1.2× larger than the slope-average values reported by SRR-CWDA-2021-00043. The cap slopes may tend to steepen rather than flatten over time as stated in SRR-CWDA-2021-00043, because mass is removed at the fastest rate just above the break in slope at the edge of the cap; eroded mass will move down the side slopes before the eroded sediment encounters a flattened slope for deposition.
- The C and K factors have substantial uncertainty (maximum C is 50× larger than the minimum and maximum K is 14× larger than the minimum). This uncertainty has a large impact on erosion rates. With these held constant at their upper bound (i.e., assuming no succession and all layers with identical soil erodibility), Figure 5.1-1 of SRR-CWDA-2021-00043 shows that a slope-average of 152.4 cm [60 in] would have been removed

after ~1,000 yrs [corresponding to 183 cm [72 in] removed at the base of the slope, or complete exposure of the GMB].

- SRR-CWDA-2021-00043 assumes the cover succession transforms from an initial grassland to fully forested over the 320 yrs starting 40 yrs after end of institutional control, based on WSRC-STI-2008-00244. The WSRC-STI-2008-00244 model was developed to estimate how rapidly tree roots might be present and form a means of damaging the GMB; in that context, rapid reforestation is conservative. The WSRC-STI-2008-00244 model represents reforestation as an encroachment process, with seeds falling within a limited distance from a mature tree. DOE assumed that reforestation cannot start until seeds migrate up the rip-rap–covered side slopes, so the timing and location of reforestation initiation on the cap has considerable uncertainty. This reforestation model implies that any point on the cap will start as grassland and have a relatively short transition in cover properties over a few decades as the first seeds at the location mature into trees. In other words, during the transition some of the cap is grassland and some of the cap is forested. According to the WSRC-STI-2008-00244 reforestation model, the area of connected grassland will gradually shrink until final colonization is complete. Accordingly, a conservative assessment of erosion potential would use a value of C that is representative of grassland (not transitional woodland shrub) in the connected grassland swaths until colonization is complete because of the associated greater erosion.
- SRR-CWDA-2021-00043 assumes that the cap uses the most erodible local soil for topsoil and backfill. While conservative, other local options are available that may substantially reduce estimated erosion rates, and it may be useful to select a less erosive option. It is also important to ensure that the backfill has lower erodibility than the topsoil; otherwise, locations where the backfill is first exposed will tend to erode even faster, starting a feedback process that may lead to gullies.

Gully potential

Gullies represent local zones that concentrate flow; thus, the cover may locally erode more quickly than estimated with the sheet and rill analysis. Sufficiently rapid erosion may expose the composite barrier at the base of the lateral drainage layer in the cap. SRR-CWDA-2021-00076 evaluates the uncertainties on infiltration for the FTF and HTF caps using the underlying approach and numerical models developed by Gustitus and Benson (SRRA162682-000002, 2020). Gustitus and Benson (SRRA162682-000002, 2020) consider potential impacts on inflow through the FTF and HTF caps due to gullies penetrating to the composite barrier, showing that infiltration may greatly increase due to gullies. SRR-CWDA-2021-00076 does not use gully infiltration based on the SRR-CWDA-2021-00043 assessment that gullies are not expected on the FTF and HTF caps.

SRR-CWDA-2021-00043 assesses the potential for gullying using a stability analysis based on the ratio of the actual velocity V_a to the permissible velocity V_p. When $V_a < V_p$ during the PMP, then the surface is assumed stable with respect to potential gullying.

The actual velocity V_a is defined as the flow velocity during a PMP event and the permissible velocity V_p is defined as the maximum flow velocity without significant sediment attachment (determined based on a vegetation-dependent maximum permissible velocity multiplied by a depth-dependent velocity correction factor, CF). Maximum flow velocity is estimated as the ratio of the peak flow rate to the flow depth, where peak flow rate is determined using the Rational Method formula and flow depth is estimated using the Manning equation.

The Rational Method formula is:

$$Q = F\ C\ I\ A$$

where Q is the peak flow rate, F is a flow concentration factor, C is a runoff coefficient, I is rainfall intensity, and A is drainage area. Note that the A and C symbols in the Rational Method formula differ from the parameters using those symbols in the RUSLE formula.

The F factor was assigned 2.5, between concentrated flow (2) and channelized flow (3), reduced from the guidance-recommended 3 to account for channel vegetation (note SRR-CWDA-2021-00036 assigned the F factor a value of 3). The C factor was assigned a value of 0.38 to be representative of low relief with normal infiltration, low vegetative cover, and a well-defined system of small drainageways. The I factor is determined by calculating the time of concentration t_c based on the channel length and slope, calculating the PMP for that duration, and dividing PMP by t_c. PMP was estimated by extrapolating PMP values for 15 min, 1 hr, and 24 hr with return periods of 1,000 and 10,000 yrs. Each PMP value was calculated in two ways: (i) using site-specific data and (ii) using regional data. These PMP values were augmented with values from two historical site sources; the analysis used the maximum PMP value among the four sources. The t_c value, A factor, and flow depth were all determined using formulas recommended by NUREG-1623. Aside from the F factor, the calculations used the same approaches as SRR-CWDA-2021-00036.

The following discussion is supplemental to the 2023 NRC Technical Reviews, based on checks of the gully erosion calculations.

- SRR-CWDA-2021-00043 Tables 5.3-1 and 5.3-2 summarize the calculations for the FTF and HTF caps, respectively. NRC staff were not able to reproduce the rainfall intensity coefficient I in these tables: the values appear to be ~2.2× larger than the corresponding equation would provide {e.g., 1500 instead of 683 mm/hr [59.1 instead of 26.9 in/hr] for the 1,000-yr PMP analysis in Table 5.3-1} and is not consistent with similar calculations in SRR-CWDA-2021-00036. Downstream-affected values include (i) the peak flow rate Q, (ii) the flow depth y, (iii) the actual flow velocity V_a, and (iv) the velocity correction factor CF, which appear to be calculated consistently with the tabulated I.
- The Manning n value of 0.235 selected in SRR-CWDA-2021-00043 appears to be non-conservative. Even assuming a very weedy, heavy stand of timber and underbrush for a minor stream, the n value ranges from 0.075 to 0.15, and once the erosion barrier is exposed, an analogous condition would be a mountain stream with gravel and cobbles, with n between 0.03 and 0.05. SRR-CWDA-2021-00036 uses a value of 0.05 to represent the SDF Closure Cap for gully erosion analyses. Note that the n value naturally fluctuates over time due to seasonal changes in growth state and events such as fires that reset the vegetation, and for gully erosion calculations it is appropriate to assume that storms occur under adverse conditions. The Manning n value affects both V_a and CF; V_a is inversely proportional to flow depth and the flow depth is proportional to the Manning n parameter raised to the power of 0.6, while CF increases with the logarithm of flow depth (Eq. 6-9 of SRR-CWDA-2021-00036). As the Manning n parameter increases, V_a decreases (the same flow rate is slower and deeper) and V_p increases (the bottom experiences less tractive force with deeper flow). V_a would increase by a factor of ~2.5× with n at 0.05 instead of 0.235.
- It is unclear why vegetation should influence the F factor because the F factor accounts for geometric concentration from the total drainage area to the channel area.

The guidance recommends 3 and SRR-CWDA-2021-00036 assigned the F factor a value of 3. However, DOE selected a value of 2.5 in SRR-CWDA-2021-00043.

- NRC confirmatory calculations switched n from 0.235 to 0.05 and C from 2.5 to 3, keeping all other parameters used in the analysis the same. V_a and V_p were not affected enough to change whether V_a is larger than V_p, but such a change may affect conclusions if a larger PMP estimate is adopted, as suggested in the 2023 Site Stability Technical Review.

SRR-CWDA-2021-00076. "Evaluation of the Uncertainties Associated with the F-Area and H-Area Tank Farm Closure Caps and Long-Term Infiltration Rates."

This report describes the development of a probabilistic model for estimating infiltration rates through the FTF and HTF closure caps for use as inputs to future FTF and HTF vadose zone flow modeling. The probabilistic model is implemented using the commercially available GoldSim modeling software. The modeling approach is largely based on a similar probabilistic closure cap model for the Saltstone Disposal Facility (SDF), described in SRR-CWDA-2021-00040. SRR-CWDA-2021-00076 (i) describes changes in the model described in SRR-CWDA-2021-00040 to account for differences in closure cap geometry and refinements to input assumptions, (ii) provides selected outputs from the probabilistic model for the FTF, HTF, and SDF caps, and (iii) provides recommended infiltration histories for the FTF and HTF Realistic, Compliance, and Pessimistic Cases.

The FTF, HTF, and SDF closure caps are all designed with a series of layers, including (i) upper earthen materials consisting of topsoil, two backfill layers sandwiching an erosion protection layer, and an Upper Lateral Drainage Layer (ULDL); (ii) a composite barrier consisting of a high-density polyurethane (HDPE) geomembrane (GMB) over a geosynthetic clay liner (GCL); and (iii) lower earthen materials consisting of a foundation layer, backfill, and the original soil (Figure 1). The FTF design uses one cap and the HTF design uses three caps (HTF-E and HTF-W caps, for the East Hill and West Hill tanks, respectively, and a small closure cap over the H-Area Pump Pits) (Figure 2); the SDF design uses two caps (one for cylindrical disposal units and one for rectangular Vaults 1 and 4). All FTF and HTF tanks have a minimum of 5.5 m [18 ft] combined cover (SRR-CWDA-2021-00076).

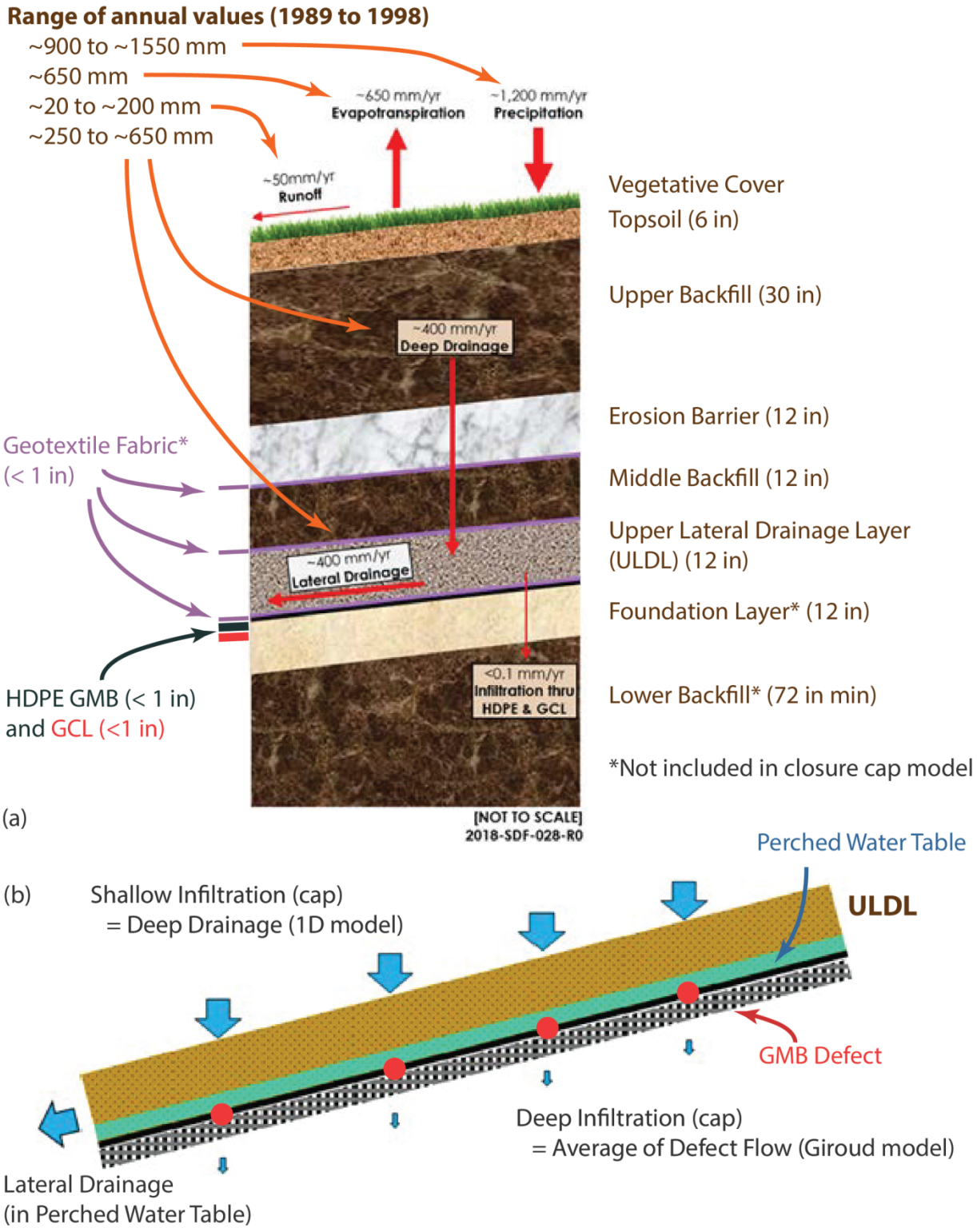

Figure 1. (a) Shallow layers in the FTF, HTF, and SDF Closure Cap, with approximate ranges of water fluxes. (b) Conceptual model for flow through the Closure Cap GMB, with the perched water draining in the ULDL driving localized flow through GMB defects. [Modified from SRR-CWDA-2019-00001 Fig. 3.2-35 and SRR-CWDA-2021-00076 Figure 2.1-2]

Figure 2. Layout of the FTF and HTF Closure Caps and a representative cross section through the HTF-E and HTF-W caps [Modified from SRR-CWDA-2021-00076 Figures 1.3-2, 1.3-5, and 1.3-6]

The underlying methodology for calculating inflow through the SDF cap is described in the DOE 2020 SDF Performance Assessment (2020 SDF PA, SRR-CWDA-2019-00001) and related documents. Benson and Benavides (SRRA107772-000009, 2018) developed the underlying analyses for the SDF cap; and Gustitus and Benson (SRRA162682-000002, 2020) adapted the same modeling approaches for the FTF and HTF caps. The calculation is performed in two steps: (i) estimating annual average drainage to the ULDL using a one-dimensional (1D) model that also considers daily precipitation, evapotranspiration, and runoff; and (ii) estimating flow through hypothetical defects using an empirical equation, given the depth of water perched in the ULDL above the GMB due to annual average drainage to the ULDL. In terms of the cap water balance, shallow infiltration refers to vertical flow above the ULDL, deep drainage is flow entering the ULDL, and deep infiltration refers to vertical flow immediately below the composite GMB/GCL barrier. The calculated defect flows from all defects are considered in estimating the deep infiltration; the averaged flow is used as the top boundary condition for detailed models of flow through and around the tanks. The perched water on the GMB is separate from the regional water table below the cap. The empirical equation for defect flow was developed for a single compacted earth layer under a defect in the GMB, with a water table in the compacted earth layer. The equation development considered flow in a saturated bulb extending from the defect to the regional water table. The water pressure at the defect is assumed based on hydrostatic pressure in the perched water table (i.e., based on the depth of the perched water). Atmospheric pressure is assumed at the base of the saturated bulb (the water table condition). For the empirical equation to be directly applicable to the cap, the water pressure must be atmospheric at the base of the GCL (the regional water table must be at the base of the GCL). In actuality, the cap GMB will be located a substantial distance above the regional water table, so the water pressure at the base of the GCL will be quite negative, and the pressure difference driving flow through the GCL will be much larger than assumed in the empirical equation.

NRC addressed the 2020 SDF analyses of percolation through the SDF cap in two technical review reports: ML23017A083, examining percolation and potential cap erosion, and ML23017A089, examining the performance of composite barrier layers and lateral drainage layers in the cap. Because of the similarity between the cap designs and the analysis approaches, the 2023 technical reviews related to the SDS cap analyses are directly relevant to the FTF and HTF cap analyses, as well.

In the SDF cap technical reviews, the NRC staff

- Found the long-term performance of the cap erosion barrier, which is responsible for protecting the ULDL and underlying composite barrier, to be risk-significant for infiltration;
- Pointed to several plausible degradation processes for the ULDL and GCL that were not included or used to calculate or simulate flows through the composite barrier (e.g., defect generation along the heat-affected zone of GMB seams, root penetrations along seams, and GCL degradation below defects);
- Found that the shallow infiltration rate estimates (i.e., flow entering the ULDL) are acceptable for deterministic modeling;
- Found that the deep infiltration rate estimates (i.e., flow passing through the composite barrier below the ULDL) were not acceptable for determining compliance because the technical bases lacked confirmatory evidence and model support to match their risk significance;
- Found that the implementation of the shallow infiltration rate abstraction for the probabilistic SDF Closure Cap Model not to be acceptable due to large uncertainties, and recommended monitoring the DOE conceptual model.

SRR-CWDA-2021-00076 (FTF and HTF caps) and SRR-CWDA-2021-00040 (SDF caps) use the underlying approach and numerical models developed by Gustitus and Benson (SRRA162682-000002, 2020) and Benson and Benavides (SRRA107772-000009, 2018) to develop inputs for probabilistic GoldSim simulations over the 10,000-yr post-closure period. Probabilistic inputs account for surface water balance components affected by meteorologic patterns (precipitation, evapotranspiration, and runoff), the effect of soil erosion on inflow to the ULDL, and degradation of the ULDL, GMB, and GCL.

Inflow to the ULDL. To facilitate the GoldSim model calculations, the numerical models developed by Gustitus and Benson (SRRA162682-000002, 2020) and Benson and Benavides (SRRA107772-000009, 2018) were used with adjusted site-specific parameters to develop empirical equations that relate model input parameters (e.g., precipitation, evapotranspiration, soil thickness) to abstracted relationships (e.g., inflow to the ULDL) (SRR-CWDA-2021-00040). Simulations were run for all combinations with three levels of precipitation condition (low, intermediate, and high), three levels of climate condition (drier, current, wetter), and four levels of soil thickness (0, 12, 24, and 36 in of soil above the erosion barrier (i.e., 36 combinations). The precipitation conditions represent the 10, 50, and 90 percentiles of a statistical distribution of observed site annual values. The climate conditions are used to scale (i) precipitation by 0.75x, 1x, and 1.25x; (ii) evapotranspiration by 0.8x, 1x, and 1.2x; and (iii) runoff by 0.5x, 1x, and 1.5x relative to current conditions; Table 1 lists the combined precipitation values.

Table 1. Precipitation Values Simulated in UNSAT-H [SRR-CWDA-2021-00040 Table 4.2-2]

Precipitation Condition	Annual Precipitation (in/yr)		
	Drier Climate Condition	Current Climate Condition	Wetter Climate Condition
High	44.9	60.3	76.2
Intermediate	36.8	49.5	62.3
Low	29.4	38.8	47.8

The equations account for complete soil removal above the erosion barrier, but this condition is not experienced with the GoldSim inputs. The SDF cap model assumed that gullying does not occur on the cap, based on the analysis from SRR-CWDA-2021-00036 showing that the SDF cap is not expected to experience gullying (SRR-CWDA-2021-00040), and this assumption tacitly stayed in the HTF and FTF models. During GoldSim sampling, the annual precipitation rates and depths of erosion (hence soil thickness) were varied based on recommendations from the Evaluation of the Potential for Erosion in the Vicinity of Z Area (SRR-CWDA-2021-00036), with the sampled values used to calculate inflow to the ULDL using the empirical relationships.

The GoldSim equations do not consider uncertainty in backfill saturated hydraulic conductivity (K_{sat}). The simulation results of Gustitus and Benson (SRRA162682-000002, 2020) and Benson and Benavides (SRRA107772-000009, 2018) have rather different simulation results (Table 2) but the same input meteorology. NRC found no discussion of what drives the different inflow and ET values for the same meteorological record but identified a small change in the K_{sat} value used for the backfill and erosion barrier as a difference between the two. Gustitus and Benson (2020) calculate runoff as no more than 8 percent of precipitation, whereas Benson and Benavides (2018) calculate runoff as no more than 15 percent of precipitation. NRC staff hypothesize the smaller K_{sat} value may keep wetting pulses nearer the top of the cap, enhancing evapotranspiration. A factor of two is a relatively small difference in K_{sat} for natural porous media.

Table 2. WINUNSAT-H Simulation Results for Calculated Drainage and Evapotranspiration

Simulation period	Gustitus and Benson (2020) K_{sat} = 5×10^{-7} m/s		Benson and Benavides (2018) K_{sat} = 1×10^{-6} m/s	
	Drainage (mm/yr)	**ET** (mm/yr)	**Drainage** (mm/yr)	**ET** (mm/yr)
Average year	200	950	400	650
Wettest decade	250	1100	525	650
Maximum inflow	360	1200	650	650

Degradation of the ULDL. The GoldSim model represents degradation of the ULDL due to silting that completely transforms the ULDL K_{sat} into the equivalent of the overlying backfill K_{sat} over a period sampled from 300 to 30,000 yrs. The initial K_{sat} is assumed to be between 5×10^{-2} cm/s [142 feet per day (fpd)] and 1.29 cm/s [3,657 fpd] with a mean of 0.15 cm/s [425 fpd]. The final K_{sat} is assumed to be sampled between the initial K_{sat} and the backfill K_{sat} {i.e., between 2×10^{-5} cm/s [0.06 fpd] and 1.4×10^{-4} cm/s [0.40 fpd] with a mean of 4.1×10^{-5} cm/s [0.12 fpd]}, based on recommendations from the *Closure Cap Model Parameter Evaluation: Saturated Hydraulic Conductivity of Sand* (SRR-CWDA-2021-00031).

Degradation of the ULDL has consequences for performance because of the effect of smaller K_{sat} on flow depths within the ULDL (i.e., the depth of the water perched above the GMB). Increased flow depths increase the head driving flow through GMB defects and may indirectly lead to erosion that exposes the GMB below the ULDL. In the Giroud solution, flow through defects is proportional to the depth of flow above the GMB raised to the power of 1.87, so defect flow will be ~29 times larger if the perched water level is the ground surface instead of the top of the ULDL. SRR-CWDA-2021-00076 evaluates defect flow at the downslope end of the ULDL, but this may not be the most conservative location when the ULDL is fully saturated.

The equation used for estimating flow depth is based on Darcy's Law, assuming steady state.

$$q_{in}A = -K(h)H\left(\frac{dh}{d\xi} + \frac{dz}{d\xi}\right)w$$

$$\frac{dh}{d\xi} \ll \frac{dz}{d\xi}$$

$$s = -\frac{dz}{d\xi}$$

where q_{in} is inflow to the ULDL, A is the upstream area, K is the lateral hydraulic conductivity in the ULDL, H is the layer thickness, h is the pressure head, z is elevation, w is the cross-sectional width, and ξ is the horizontal coordinate in the downslope direction. Assuming that (i) the gradient of h is small compared to the slope (flow is almost parallel to the base of the ULDL), (ii) the perched water is in a uniform medium (flow is entirely in the ULDL), (iii) flow is entirely below the height of the perched water ($K = 0$ above the perched water elevation, so that $K(h)H = K_{sat}h$, where K_{sat} is the saturated hydraulic conductivity in the lateral direction), and (iv) evaluation is at a slope length of L,

$$h \approx \frac{q_{in}A}{K_{sat}sw} = \frac{q_{in}L}{K_{sat}s}$$

The simplification is in error when K_{sat} is so small that the ULDL becomes fully saturated in order for all inflow to reach L ($h = H$). When the flow capacity in the overlying backfill is negligible, the ULDL slope is small relative to the head gradient and

$$\frac{dh}{d\xi} = -\frac{q_{in}L}{KH}$$

The sharper gradient means that the water table may rise high into the backfill, even potentially discharging to the cap surface. An elevated water table has consequences for the near-surface water balance because less infiltration capacity is available during precipitation events (increasing runoff), thus the changed water balance is likely to increase cap erosion rates. Furthermore, focused upwelling may provide conditions that promote localized erosion, such as gullying, that is not considered in the analysis. Once a gully is initiated, it may propagate upslope beyond the area affected by an elevated water table.

The critical value of K for which the simplification begins to be in error (K_c), occurs when the ULDL is just filled with water at the end of the slope

$$K_c = \frac{q_{in}L}{Hs}$$

For the slope lengths of the FTF and HTF caps, typical estimated inflow rates to the ULDL will generate water depths exceeding the ULDL thickness with the ULDL K_{sat} at ~0.01 cm/s [28 fpd].

The statistical parameters describing the ULDL degradation suggest that the final value for the ULDL K_{sat} has a median of ~0.011 cm/s [31 fpd] and is < 1×10^{-3} cm/s [2.8 fpd] in ~14 percent of realizations. In ~14 percent of realizations, the ULDL K_{sat} drops below 0.01 cm/s [28 fpd] within 1,000 yrs. When the K_{sat} drops below 0.01 cm/s [28 fpd] the perched water table exceeds the ULDL thickness.

In SRR-CWDA-2021-00076, DOE recommended using the geometric mean of the probabilistic simulations for infiltration boundary conditions in Realistic Case modeling and the 95th percentile estimates for infiltration boundary conditions in both the Compliance Case and Pessimistic Case modeling of individual tanks. As confirmation, the time histories of these statistical values appear to be closely related to the time histories for the transition of the ULDL K_{sat} to <0.01 cm/s [<28 fpd].

By implication, deep percolation may be underestimated for extended durations in a substantial fraction of realizations when the constriction in flow is not considered.

In addition, in the Near Field Flow and Transport TRR for the Saltstone Disposal Facility (ML23017A086), NRC staff discussed the potential for geometric averaging to significantly underestimate values and the lack of support of geometric averaging.

HDPE Uncertainty. The GoldSim model represents the performance of the HDPE GMB in terms of defects in the GMB, which allow water to pass into the underlying GCL. The GoldSim model allows three modes: (i) no failure, (ii) partial failure, and (iii) complete failure, but SRR-CWDA-2021-00076 exclusively uses the partial failure mode. The technical basis for the

parameters is developed in *Closure Cap Model Parameter Evaluation: High Density Polyethylene (HDPE) and Geosynthetic Clay Liner (GCL) Composite Barrier Performance* (SRR-CWDA-2021-00033, Revision 1).

In the partial failure mode, the defects are represented as an initial (sampled) number of defects that evolve over time. The defect size is described with two sampled parameters, the initial size, and the HDPE service life. After half the sampled service life has elapsed, the defect area is assumed to grow exponentially until the end of the simulation. The doubling interval is set at half the service life (i.e., the defect area doubles from $0.5T_{SL}$ to T_{SL} and doubles again by $1.5T_{SL}$, where T_{SL} is the sampled service life). The model assumes that the impact of potential new defects is captured by the enlargement of the initial defects. Stress cracks are assumed to have no impact on inflow, in contrast to the Gustitus and Benson (SRRA162682-000002, 2020) model for the FTF and HTF closure cap.

SRR-CWDA-2021-00033 reviews information from the literature to develop the basis for the sampled parameters. The number of initial defects is represented with a lognormal distribution with a mean of 4 defects/hectare and standard deviation of 6.5 defects/hectare based on the recommendation of Giroud and Bonaparte (1989). The diameter of initial defects is represented as log-uniform between 0.1 mm [3.9×10^{-3} in] and 11.3 mm [0.44 in] {i.e., the median diameter is ~1 mm [0.04 in]}, based on an interpretation step that samples a distribution of defect sizes before and after repair from the literature. Note that the GoldSim model assumes that all defects have the same size in any given realization, instead of sampling a population of defects with various sizes.

SRR-CWDA-2021-00033 uses a lognormal distribution with mean of 1,975 yr and standard deviation of 1,200 yr to represent the service life distribution of the SDF closure cap {a 1.5-mm [5.9×10^{-2} in] HDPE GMB at 22 °C [71.6 °F]}. The mean service life is based on the minimum service life estimates from Tian et al. (2017), which were developed for one-sided degradation of 2-mm [7.9×10^{-2} in] HDPE GMB at 15 °C [59 °F]. The SRR-CWDA-2021-00033 analysis considers corrections for temperature, test water quality, one-sided versus two-sided immersion testing, and uncertainties regarding the definition of service life (several degradation criteria have been used to define service life).

The standard deviation of the service life distribution was selected to include a lower range calculated by Rowe (2005) and an upper range calculated by increasing the Tian et al. (2017) estimates based on the milder chemical characteristics of site water compared to the experimental water.

The service life calculations are intended to represent the conditions experienced far from an existing defect, because of the assumption of one-sided exchanges. The GMB next to a defect is likely to have flow washing the inside of the defect and the top and bottom of the GMB (i.e., three-sided exchanges), however, which will locally accelerate degradation near the defect.

NRC staff provide the following context. Inflow is proportional to the defect area raised to the power of 0.1 in the Giroud solution used to estimate flow through defects. The defect area is assumed to double on a fixed interval equal to half the service life. With the Giroud solution, increasing the size of the defect by a factor of 1,024 (doubling the defect area 10 times) will increase calculated inflow by a factor of 2, all else equal. In contrast, the average inflow is proportional to the number of defects. The inflow will change by 1.6× over the 100-fold range for the assumed initial defect size, all else equal. The average inflow will increase by 70 times over the range from the 5th to the 95th percentile (0.25 to 17.6 defects/hectare) of the assumed distribution for initial defects, all else equal.

This comparison suggests that the doubling strategy for increasing defect area over time does not at all represent the effect of increasing the number of defects over time.

HDPE-to-GCL Contact Factor. NRC staff note that the Giroud solution was developed for a scenario with a GMB contacting a low-permeability earthen medium extending to the water table. The contact factor in the Giroud solution accounts for lateral flow between the GMB and underlying medium. In the original context, the contact factor accounted for physical gaps between the GMB and earthen medium. In the context of a GCL, the contact factor also accounts for potential lateral flow in the GCL geotextile above the clay layer.

The GoldSim model represents the contact factor between the HDPE and GCL as a constant that represents good contact, based on the assumption that the conceptual design ensures good contact (flat installation, compressive stress from overburden, bentonite slurry extrusion from the GCL). Rowe (2020) tabulates several studies of interface transmissivities that range between 6×10^{-12} to 4×10^{-10} m^2/s for water with moderate normal stress. For comparison, the corresponding transmissivity for a 0.01-m GCL with initial K_{sat} of 1×10^{-11} m/s is 1×10^{-13} m^2/s, implying that substantially more flow can be carried in the geotextile than in the clay. It is not clear that the assumed contact factor appropriately accounts for this lateral flow.

GCL Uncertainty. The GoldSim model represents the performance of the GCL with distributions for the GCL thickness, the GCL initial K_{sat}, and a degradation multiplier. The degradation multiplier is applied based on the HDPE service life, T_{SL}, ramping from $0.5T_{SL}$ to T_{SL} (i.e., the initial value isw assumed to hold until the HDPE begins to deteriorate). The technical basis for the parameters is developed in SRR-CWDA-2021-00033. These parameters are used to calculate inflow through a GMB defect, using the Giroud solution.

NRC staff note that the Giroud solution calculates inflows that are proportional to the GCL K_{sat} raised to the power of 0.74 and approximately inversely proportional to the GCL thickness.

The GCL thickness is represented as a normal distribution with mean of 8.5 mm [0.33 in] and standard deviation of 1.5 mm [0.06 in], based on values for wetted thickness from the literature.

The GCL initial K_{sat} is represented as a log-triangular distribution with minimum, mode, and maximum values of 1.4×10^{-11}, 1×10^{-9}, and 4×10^{-7} cm/s [4×10^{-8}, 3×10^{-6}, and 1×10^{-3} fpd], respectively. These values are developed using recommendations and measurements from Rowe (2012), reduced by a factor of 5 to account for measured values at an analog site in Barnwell, South Carolina.

The GCL K_{sat} multiplier is represented as a log-triangular distribution with minimum, mode, and maximum values of 1, 10, and 354, respectively. These values are based on (i) data obtained from the Barnwell analog site showing little change in K_{sat} after 14 yrs, (ii) inferences regarding cation exchange processes with low-ionic-strength waters, (iii) and assumptions that dehydration, freeze-thaw, and wetting-drying processes will be negligible at the site. The upper bound is based on generic recommendations from NUREG/CR-7028 (ML12005A110) for long-term cation exchange in the absence of dehydration, scaled-up to account for uncertainty. The combination of initial K_{sat} and multiplier results in a final K_{sat} distribution between 1.4×10^{-11} and 1.4×10^{-4} cm/s [4×10^{-8} and 0.4 fpd].

NRC staff note that SRR-CWDA-2021-00033 cites Rowe (2012) as recommending different GCL K_{sat} values based on confining pressure, without discussing corrections for site-specific overburden pressure. Rowe (2012) recommends initial GCL K_{sat} values of 5×10^{-9}, 1×10^{-9}, and 7×10^{-10} cm/s [1.4×10^{-5}, 2.8×10^{-6}, and 2.0×10^{-6} fpd] for overburden pressures of 3 to 4 kPa [0.44 to 0.58 psi], 34 to 38 kPa [4.93 to 5.51 psi], and 109 to 117 kPa [15.8 to 17.0 psi], respectively. For a bulk overburden density of 1200 kg/m^3 [75 lbs/ft^3], these correspond to a thickness of 0.26 to 0.34 m [0.85 to 1.1 ft], 2.9 to 3.2 m [9.5 to 10.5 ft], and 9.3 to 9.9 m [30.5 to

32.5 ft], respectively. For the FTF and HTF caps, the overburden thickness above the GCL is ~2 m [~6.6 ft], thus the 1×10^{-9} cm/s [2.8×10^{-6} fpd] value (corresponding to the Barnwell data) appears justified. It does not appear justified to impose a lower bound for initial GCL K_{sat} that is nearly two orders of magnitude smaller than 1×10^{-9} cm/s [2.8×10^{-6} fpd].

NRC staff note that the upper bound value taken from Rowe (2012) represents calculations based on immersion in an aggressive synthetic leachate, which is not expected to be representative of the initial (or long-term) conditions in the FTF and HTF cap environment.

SRR-CWDA-2021-00033 acknowledges that GCLs not covered by GMBs or subject to dry conditions may become much more permeable over time, attributing such increased GLC K_{sat} values to loss of swelling capacity coupled with the formation of cracks from dehydration or freeze–thaw cycles. SRR-CWDA-2021-00033 argues that loss of swelling capacity is the largest driver for GCL K_{sat} degradation because (i) freeze–thaw cycles are not expected at the site and (ii) wet–dry cycles with deionized water have been shown to have little impact on GCL K_{sat}.

NRC staff note that there is little or no data obtained for the evolution of GCL K_{sat} for locations under a defect, and the most representative data may be for GCLs not covered by GMBs. Scalia and Benson (2011) and Scalia et al. (2017) report measured K_{sat} values for GCL samples $>1 \times 10^{-4}$ cm/s [0.3 fpd] in exposed locations or with low water content, and 1×10^{-5} cm/s [0.03 fpd] for samples with observed penetrations (fast pathways associated with clumped needle-punched fibers). Further, the GCL will be located far above the water table, thus is likely to dehydrate over time. SRR-CWDA-2021-00033 does not discuss penetrations or how the GCL will maintain hydration. These data, obtained from exhumed GCLs, suggest that the GCL K_{sat} under defects may evolve to the assumed upper bound for degraded GCL within years to decades.

Discussion

The GoldSim model discussed in SRR-CWDA-2021-00076 largely follows the models developed by Benson and Benavides (SRRA107772-000009, 2018) and Gustitus and Benson (SRRA162682-000002, 2020), with the subsequent detailed analysis of input parameters of SRR-CWDA-2021-00040. The model-calculated inflows appear to be most sensitive to (i) pressure head in the ULDL as influenced by inflow to the ULDL and ULDL K_{sat}, (ii) number of GMB defects, and (iii) GCL K_{sat}.

NRC staff recognize that the inflow calculations are strongly dependent on the assumptions in the Giroud solution, which was developed to represent a GMB defect over a low-permeability earthen barrier extending to the water table. The composite barrier in the FTF and HTF closure caps differs from these assumptions in two key ways: (i) the GCL includes a geotextile layer potentially allowing enhanced lateral flow above the clay layer, and (ii) the composite barrier has an extensive underlying backfill extending to the water table. Further, the GoldSim model does not consider the impact of preferential conditions that are likely to enhance flow near defects (e.g., seams, cracks, dehydration). Accordingly, NRC staff considers there to be a potentially large amount of model uncertainty in addition to the parameter uncertainties addressed in the GoldSim model.

An independent analysis was performed that addresses some of these issues using separate numerical modeling approaches. This analysis suggests that:

- Accounting for lateral flow, variable saturation, and GCL degradation processes yields inflow estimates with substantially different sensitivities than are found in the Giroud solutions used to estimate defect inflow. In particular, (i) explicitly accounting for lateral flow above the GCL tends to reduce the sensitivity to perching height and (ii) explicitly accounting for the depth to the water table (e.g., using pressure conditions on the base

of the GCL based on hydrostatic equilibrium with the regional water table) tends to increase defect inflow. Neither modeling approach is unequivocally conservative for all combinations of parameters.

- The parameter values used to describe GMB and especially GCL degradation appear to be optimistic for site conditions.
- Reasonable alternative model approaches and parameter assessments would generate expected inflows (i) within decades that are comparable to "highly unlikely" rates recommended by Gustitus and Benson (SRRA162682-000002, 2020) for periods after 1,000 yrs and (ii) within centuries that are comparable to "highly unlikely" rates recommended for periods after 2,000 yrs. The alternative model estimates are comparable to the maximum probabilistic HTF inflow developed by SRR-CWDA-2021-00076 and somewhat less conservative than previous HTF PA inflow estimates.
- Much of the uncertainty in inflow arises from uncertainty in GCL performance. The model used for the FTF and HTF cap assumes that the GCL slightly degrades and largely neglects lateral flow between the GMB and GCL. In contrast, independent analysis suggests that the designed GCL will likely desiccate (it is far above the water table) and may experience potential wet and dry cycles near defects, promoting creation of fast connected pathways along the top of the GCL that connect to vertical fast pathways bypassing the clay matrix (e.g., through fiber bundles).
- Future development of new defects is a second source of substantial uncertainty. The methodology used in SRR-CWDA-2021-00076 (increasing the size of initial defects) has much less influence on inflows than considering new defects and cracks, especially along seams.
- A conceptual model that considers defect-based inflow is likely to be characterized by large zones with minimal flow that are interspersed with highly localized enhanced flow conditions. Therefore, widely dispersed "average" flow conditions may not be representative of the real system. Average calculated tank releases may be different for (i) a scenario where a few tanks are inundated and the remainder are dry, compared to (ii) a scenario where all tanks receive an average inflow rate.
- The ULDL appears to be inadequate to convey expected inflow if moderate degradation from silt redistribution is assumed (e.g., a reduction in the ULDL K_{sat} to <0.01 cm/s [<28 fpd]). Inadequate capacity will tend to reduce infiltration, create wet spots on the cap, and promote runoff with associated cap erosion.

Suggested Design Considerations

Two relatively simple changes to the cap design may greatly reduce uncertainties in cap performance.

- Increasing the ULDL thickness near the outlet of the ULDL may provide an increased factor of safety with respect to changes in flow depth stemming from K_{sat} degradation in the ULDL. It may be adequate to have a thinner ULDL near the cap crest to reduce the need for additional material.
- NRC staff recommend that DOE consider methods to protect the base of the GCL (e.g., with a HDPE coating on the base geotextile or with an underlying GMB that will not negatively impact cover performance) to reduce uncertainties about the model approach, parameters, and potential fast pathways through the GCL for extended durations.

REFERENCES

AbdelRazek, A.Y., and R.K. Rowe. “Interface transmissivity of conventional and multi-component GCLs for three permeants.” *Geotextiles and Geomembranes*. Vol 47, No. 1, pp. 60–74. doi:10.1016/j.geotexmem.2018.10.001. 2019.

Giroud, J., and R. Bonaparte. “Leakage Through Liners Constructed with Geomembranes—Part I.” *Geotextiles and Geomembranes*. Vol 8, No. 1, pp. 27–67. doi:10.1016/0266-1144(89)90009-5. 1989.

IEI 2024-001. Denham, M.E. “Opportunities to Update the Model of Tank Closure Grout Aging (SRNL-STI-2012-00404) Based on Experimental Results by the Savannah River Ecology Laboratory. Columbia, Maryland: Inspection Experts, Inc. February 2021. [ADAMS Accession No. ML22090A005]

IEI 2024-002. Denham, M.E. “Recommended Updates to Solubility Controls for Modeling Leaching of Technetium, Uranium, Neptunium, Plutonium, and Iodine from the Residual Waste Layer of Closed Savannah River Site High-Level Waste Tanks.” Columbia, Maryland: Inspection Experts, Inc. February 2021. [ADAMS Accession No. ML22090A006]

K-CLC-G-00111. Hasek, M.J., and R.J. Williams “Calculation Sheet: Slope Stability Analysis for the F-Tank Farm and H-Tank Farm Closure Caps.” Aiken, South Carolina: Savannah River Site, March 2021. [ADAMS Accession No. ML21196A050]

Langton, C.A., M.G. Serrato, J.K. Blankenship and W.B. Griffin. “Savannah River Site R-Reactor Disassembly Basin In-Situ Decommissioning—10499.” Phoenix, Arizona: Waste Management Conference. March 7–11, 2010.

Langton, C.A., D.B. Stefanko, M.G. Serrato, J.K. Blankenship, W.B. Griffin, J.T. Long, J.T. Waymer, D. Matheny, and D. Singh. “Use of Cementitious Materials for SRS Reactor Facility In-Situ Decommissioning—11620.” Phoenix, Arizona: Waste Management Conference. February 27–March 3, 2011.

ML21026A012. “Summary of December 9, 2020, Webinar Call Related to Experiments Conducted by the Savannah River Ecology Laboratory and the Center for Nuclear Waste Regulatory Analyses to Support Tank Farm Closure at the Savannah River Site.” Washington, DC: U.S. Nuclear Regulatory Commission. January 26, 2021. [ADAMS Accession No. ML21026A012]

ML23017A083. Arlt, H. “Technical Review: Percolation Through and Potential Erosion near the Closure Cap of the U.S. Department of Energy 2020 Performance Assessment for the Saltstone Disposal Facility at the Savannah River Site.” Washington, DC: U.S. Nuclear Regulatory Commission. April 2023. [ADAMS Accession No. ML23017A083]

ML23017A089. Arlt, H. and S. Stothoff. “Technical Review: Performance of the Composite Barrier Layers and Lateral Drainage Layers of the U.S. Department of Energy 2020 Performance Assessment for the Savannah River Site Saltstone Disposal Facility.” Washington, DC: U.S. Nuclear Regulatory Commission. April 2023. [ADAMS Accession No. ML23017A089]

ML23017A114. Alexander, H. et al. “Technical Review: Site Stability at the U.S. Department of Energy Savannah River Site Saltstone Disposal Facility (Technical Report).” Washington, DC: U.S. Nuclear Regulatory Commission. April 2023. [ADAMS Accession No. ML23017A114]

NUREG-1623. Johnson, T.L. “Design of Erosion Protection for Long-Term Stabilization (Final Report).” Washington, DC: U.S. Nuclear Regulatory Commission, September 2002. [ADAMS Accession No. ML052720285]

NUREG/CR-7028. Phillip, J. et al. “Engineered Covers for Waste Containment: Changes in Engineering Properties and Implications for Long-Term Performance Assessment.” Washington, DC: U.S. Nuclear Regulatory Commission. December 2011. [ADAMS Accession No. ML12005A110]

Park, B., S.Y. Jang, J.-Y. Cho, and J.Y. Kim. “A novel short-term immersion test to determine the chloride ion diffusion coefficient of cementitious materials.” *Construction and Building Materials.* Vol. 57, pp. 169–178. 2014. doi:10.1016/j.conbuildmat.2014.01.086.

Rowe, R.K. “Long-term performance of contaminant barrier systems.” *Géotechnique.* Vol. 55, No. 9, pp. 631–678. November 2005. doi:10.1680/geot.2005.55.9.631.

Rowe, R.K. “Short- and Long-Term Leakage through Composite Liners.” *Canadian Geotech. J.* Vol. 49, pp. 141–169. January 2012. doi:10.1139/T11-092.

Scalia, J., and C. Benson. “Hydraulic Conductivity of Geosynthetic Clay Liners Exhumed from Landfill Final Covers with Composite Barriers.” *J. Geotech. Geoenviron. Eng.* Vol. 137, No. 1, pp.1–13, 2011. doi:10.1061/(ASCE)GT.1943-5606.0000407.

Scalia, J., C.H. Benson, W.H. Albright, B.S. Smith, and X. Wang. “Properties of Barrier Components in a Composite Cover after 14 Years of Service and Differential Settlement.” *J. Geotech. Geoenviron. Eng.* Vol. 143, No. 9, 2017. doi:10.1061/(ASCE)GT.1943-5606.0001744.

SRNL-STI-2010-00035. Langton, C.A. “Chemical Degradation Assessment for the H-Area Tank Farm Concrete Tanks and Fill Grouts.” Revision 0. Aiken, South Carolina: Savannah River National Laboratory. January 29, 2010. [ADAMS Accession No. ML20206L143]

SRNL-STI-2010-00047. Garcia-Diaz, B.L. “Life Estimation of High Level Waste Tank Steel for H-Tank Farm Closure Performance Assessment.” Aiken, South Carolina: Savannah River National Laboratory. March 2010. [ADAMS Accession No. ML111220407]

SRNL-STI-2012-00404. Denham, M.E. and M.R. Millings. “Evolution of Chemical Conditions and Estimated Solubility Controls on Radionuclides in the Residual Waste Layer during Post-Closure Aging of High-Level Waste Tanks.” Revision 0. Aiken, South Carolina: Savannah River Site. August 2012. [ADAMS Accession No. ML13078A192]

SRNL-STI-2019-00009. Lorier, T.H. and Langton, C.A. “Review of Cementitious Materials Development and Applications that have Supported DOE-EM Missions: Waste Treatment, Conditioning, Containment Structures, Tank Closures, Facility Decommissioning, Environmental Restoration, and Structural Assessments.” Revision 0. Aiken, South Carolina: Savannah River Site. May 2019. doi:10.2172/1527156.

SRR-CWDA-2019-00001. Folk, J. “Performance Assessment for the Saltstone Disposal Facility at the Savannah River Site.” Aiken, South Carolina: Savannah River Site. March 2020. [ADAMS Accession No. ML20190A056]

SRR-CWDA-2021-00031. Hommel, S.P. “Closure Cap Model Parameter Evaluation: Saturated Hydraulic Conductivity of Sand.” Revision 1. Aiken, South Carolina: Savannah River Site. May 2021. [ADAMS Accession No. ML21160A061]

SRR-CWDA-2021-00033. Hommel, S.P. “Closure Cap Model Parameter Evaluation: High Density Polyethylene (HDPE) and Geosynthetic Clay Liner (GCL) Composite Barrier Performance.” Revision 1. Aiken, South Carolina: Savannah River Site. May 2021. [ADAMS Accession No. ML21160A062]

SRR-CWDA-2021-00036. Hommel, S.P. “Evaluation of the Potential for Erosion in the Vicinity of Z Area.” Aiken, South Carolina: Savannah River Site. June 2021. [ADAMS Accession No. ML21160A063]

SRR-CWDA-2021-00040. Hommel, S.P. “Evaluation of the Uncertainties Associated with the SDF Closure Cap and Long-Term Infiltration Rates.” Aiken, South Carolina: Savannah River Site. June 2021. [ADAMS Accession No. ML21160A064]

SRR-CWDA-2021-00076. Hommel, S.P. “Evaluation of the Uncertainties Associated with the F-Area and H-Area Tank Farm Closure Caps and Long-Term Infiltration Rates.” Revision 1. Aiken, South Carolina: Savannah River Site. June 2021. [ADAMS Accession No. ML23087A009]

SRRA107772-000009. Benson, C.H., and J.M. Benavides. “Predicting Long-Term Percolation from the SDF Closure Cap.” Report No. GENV-18-05, University of Virginia School of Engineering. April 2018. [ADAMS Accession No. ML20206L138]

SRRA162682-000002. Gustitus, S.A, and C.H. Benson. “Predicting Long-Term Percolation from the HTF and FTF Closure Caps.” Report No. GENV-20-09. University of Virginia School of Engineering. June 2020.

Tian, K., C. Benson, J. Tinjum, and T. Edil. “Antioxidant Depletion and Service Life Prediction for HDPE Geomembranes Exposed to Low-Level Radioactive Waste Leachate.” *J. Geotechnical and Geoenvironmental Engineering.* Vol. 143, No. 6, 2017. doi:10.1061/(ASCE)GT.1943-5606.0001643.

USDA-HDBK-703. Renard, K.G. et al. “Predicting Soil Erosion by Water: A Guide to Conservation Planning with the Revised Universal Soil Loss Equation (RUSLE).” Agriculture Handbook Number 703. Washington, DC: United States Department of Agriculture. January 1997.

WSRC-STI-2007-00061. Subramanian, K.H. “Life Estimation of High Level Waste Tank Steel for F-Tank Farm Closure Performance Assessment.” Revision 2. Aiken, South Carolina: Savannah River Site. June 2008. [ADAMS Accession No. ML111240593]

WSRC-STI-2007-00607. Langton, C.A. “Chemical Degradation Assessment of Cementitious Materials for the HLW Tank Closure Project.” Revision 0. Aiken, South Carolina: Savannah River Site. September 14, 2007. [ADAMS Accession No. ML081330358]

WSRC-STI-2008-00244. Jones, W. and M. Phifer. “Saltstone Disposal Facility Closure Cap Concept and Infiltration Estimates.” Aiken South Carolina: Savannah River National Laboratory. 2008. [ADAMS Accession No. ML083400069]

Appendix A
Summaries of Minor Reports

Consideration of Slag-free Alternative Tank-Fill Grouts (summaries in chronologic order)

SRR-CWDA-2015-00109. "DOE/SRR Liquid Waste Operations Quarterly FFA Update (Tank 16 Grouting Update—Slides)." Aiken, South Carolina: Savannah River Remediation. August 19, 2015.

Slides 5 and 6 of this presentation considered use of four flowable alternative grouts for filling the upper portion of Tank 16H after reducing tank grout had mounded below installed tremie pipes. The four flowable alternative grouts considered were equipment grout, cooling coil grout, high-flow Controlled Low-Strength Material (HF CLSM) and Saltstone Vault 4 clean cap grout. HF CLSM was not selected for placement inside the upper portion of Tank 16H because the mix was known to produce bleedwater (implying it was not the Zero-Bleed CLSM mix ZB-FF-8-D, discussed in following related summaries) and did not offer reducing capacity (due to its lack of ground granulated blast furnace slag). Based on this information, the unspecified HF CLSM considered as a flowable alternative tank fill grout for potential use in Tank 16H by DOE may have been CLSM mix EXE-X-P-0-X, discussed in following related document summaries.

C-SPS-G-00096. Baldwin, G.R. "Designing, Furnishing and Delivery of Ready Mixed Concrete, Grout and CLSM (GS & Procurement Specification)." Revision 3. September 9, 2015. [ADAMS Accession No. ML21139A041]

This is a procurement specification for Savannah River Site concrete, grout, and Controlled Low-Strength Material (CLSM), which is associated with design change forms C-DCF-G-00397 and C-DCF-G-00400, including mixes under consideration by DOE as slag-free, non-reducing, alternative tank-fill grouts. Supplier of ready-mixed concrete, grout and CLSM shall design, adjust, and qualify the various cementitious material mixes to achieve desired attributes (e.g., compressive strength, slump, material components and air entrainment) using fine and coarse aggregate available locally near the point of production, unless specified otherwise. Moisture content of fine and coarse aggregates used should be monitored and recorded, and mix water quantity should be adjusted, accordingly. Mix temperatures should not exceed 32 °C [90 °F] at the point of delivery. All design mixes should be tested at a temperature within 5.6 °C [10 °F] of the maximum allowable temperature. Documentation (i.e., Batch Tickets) should be provided that identifies the material components by brand, type, class, grade, or source of the material components corresponding to Supplier material identification numbers for the material components. Batch tickets provided by suppliers to support traceability should be legible to end-users who monitor operations. Section 3.2.2 of the specification specifies various design mixes and refers the reader to Attachment 5.3 and tables of Attachment 5.5. Once the supplier has had a design mix approved such that it becomes a production mix, adjustments to the production mix, material components of the production mix, and the source of material components of the production mix may not be made without prior approval from Savannah River Nuclear Solutions (SRNS). New adjustments and changes cause a new cementitious material mix to revert to being an unapproved design mix that must be qualified and resubmitted to SNRS for acceptance. Section 3.2.2.2 of the specification concerns concrete, including Low-Slump Concrete (mix A2000-6-0-2-A) proposed for use to seal diversion box sumps. Section 3.2.2.3.8 pertains to low shrinkage grout and extended set, low-shrinkage grout design mixes, which may be of interest to tank grouting operations that seek to minimize development

of preferential flow pathways through tank grout. Section 3.2.2.4 concerns CLSM, including mix EXE-X-P-0-X (i.e., “Common CLSM”), which has been considered for potential use as a future flowable tank closure grout (SRR-CWDA-2015-00109; SRR-CWDA-2020-00045; SREL Doc. R-21-0001). Section 3.2.2.5 of the specification concerns Zero-Bleed, Structural Flowable Fill Concrete with No. 8 stone, ZB-FF-8-D, also known as Zero-Bleed CLSM (ZB-CLSM). This mix was used to fill ancillary equipment at the F-Area Tank Farm, namely FDB-5 and FDB-6. ZB-CLSM is similar to but not the same as a slag-free, non-reducing LP#8-16 tank grout, because ZB-CLSM has a larger water-to-cementitious materials (*w:cm*) ratio and different proportions of cementitious materials (SRR-CWDA-2020-00061; SRR-CWDA-2021-00034). This procurement specification contained incorrect admixture information for ZB-FF-8-D, which was then corrected in Design Change Form C-DCF-G-00400, summarized later in this section. To clarify specific grout mixes discussed in this procurement specification and subsequent reports on slag-free, non-reducing, alternative tank-fill grouts, Table 3.5-1 of SRR-CWDA-2021-00034 is reproduced here:

Ingredient	LP#8-16 Grout (TFG)	TFG-NBFS	ZB-FF-8-D Grout	Common CLSM	Clean Cap Grout
Cement (lbs/yd^3)	125	125	150	50	193
Slag (lbs/yd^3)	210	–	–	–	867
Fly Ash (lbs/yd^3)	363	573	500	600	867
Sand (lbs/yd^3)	1790	1790	1850	2515	–
Gravel (lbs/yd^3)	800	800	800	–	–
Water (gal)	48.5	48.5	50.0	66	116
water/cement mass ratio	0.58	0.58	0.64	0.85	0.50

Section 4.4 of this specification concerns inspection/testing requirements for production mixes, also addressed in Attachment 5.4. Compressive strength cylinders of various diameters and lengths require variable numbers of cylinders to be cast. For example, one cylinder may be tested at 7 days, two cylinders at 28 days, with two cylinders placed on hold. If early compressive strength requires verification, an additional cylinder may be cast to ensure strength test requirements are met. If the 28-day compressive strength test meets design requirements, cylinders placed on hold may be discarded, unless required for testing at 90 days due to the mix containing pozzolan (e.g., Class F fly ash by SEFA Group, Wateree, South Carolina).

C-DCF-G-00397. “Populate Mix Design Tables, Attachment 5.5” (Design Change Form). November 19, 2015. [ADAMS Accession No. ML21139A044]

This Design Change Form is associated with Specification C-SPS-G-00096, Revision 3, summarized hereafter, because the original Attachment 5.5, pages 1–4 were incomplete for many Mix Design Tables. The associated change was to populate the mix design tables for various concretes, grouts, and CLSM. An important aspect of this document is the following list that provides mix component descriptions and sources (i.e., vendors and vendor locations)

(9) Mix Component Descriptions and Sources.

(9a) Cement is Type I/II by Argos from Harleyville, South Carolina

(9b) Potable water from the City of Jackson, SC Municipal Water Supply

(9c) Sand is supplied by South Carolina Minerals (SCM) located in Beech Island, South Carolina

(9d) Pozzolan is Class F by SEFA Group located in Wateree, South Carolina

(9e) 3/8" coarse aggregate is supplied by Aggregates USA from Dogwood Quarry #8 located in Appling, Georgia

(9f) 3/4" coarse aggregate is supplied by Aggregates USA from Dogwood Quarry #67 located in Appling Georgia

(9g) 3/4" coarse heavyweight aggregate for the shielding concrete is Vulcan Materials Company, #67 from the Pineville Quarry in Charlotte, North Carolina.

(9h) Retarding Admixture is Daratard 17 Type B & D and Recover Type D by W. R. Grace

(9i) Water Reducing Admixture is WRDA 35 Type A & D and Mira 85 Type A & F by W. R. Grace

(9j) Air-Entraining Admixture is Darex II by W. R. Grace

(9k) High Range Water Reducing admixture is Adva 380 Type F and Adva Cast 575 Type A & F by W. R. Grace

(9l) Viscosity Modifier Admixture (VMA) is EXP 958 Type S & F by W. R. Grace

C-DCF-G-00400. Blankenship, J.K. "Revise 'Designing, Furnishing and Delivery of Ready Mixed Concrete, Grout and CLSM (U)' Specification (Design Change Form)." Revision 0. February 28, 2018. [ADAMS Accession No. ML21139A043]

This Design Change Form is associated with Specification C-SPS-G-00096, Revision 3, summarized hereafter, because the original specification contained incorrect admixture information for Zero-Bleed, Structural Flowable Fill Concrete with No. 8 stone (ZB-FF-8-D). The viscosity modifying admixture is WR Grace EXP-958 in the amount of 1.6 L/cubic meter [41.25 oz/cubic yard]; the high-range water reducer is WR Grace Adva® Cast 575 in the amount of 3.2 L/cubic meter [80 oz/cubic yard], and the set accelerator is a maximum of 49.9 L/cubic meter [10 gal/cubic yard], but the base case for ZB-FF-8-D is that no set accelerator is used, and the amount added depends on the desired set time. Approved set accelerators include WR Grace DCI, which is compatible with the high-range water reducer used in this mix. The amount of water in the set accelerator must be subtracted from the amount of mixing

water added.

TABLE 3: PRODUCTION STRUCTURAL FLOWABLE FILL ZERO BLEED CONCRETE

MIX OPTION	FUNCTIONAL CLASS	MIX IDENTIFIER	FLOW/SLUMP (INCHES) WORKING RANGE	FLOW/SLUMP (INCHES) IN ADV	WEIGHT OF INGREDIENTS, #/CY CEMENT	GAL/CY WATER	WEIGHT OF INGREDIENTS, #/CY SAND	WEIGHT OF INGREDIENTS, #/CY POZZOLAN	MAX AGGREGATE SIZE 3/8 IN	MAX AGGREGATE SIZE 3/4 IN	MAX AGGREGATE SIZE 1-1/2 IN	ADMIXTURES OZ/CY (UNO) RA	ADMIXTURES OZ/CY (UNO) WRA	ADMIXTURES OZ/CY (UNO) AEA	ADMIXTURES OZ/CY (UNO) SET ACCELERATOR gal/ CY (12)	RANGE HRWR OZ/CY MAX(9k)	RANGE VMA OZ/ CY (9l)	GENERAL GUIDE (SEE DESIGN DRAWINGS FOR CLASS OF CONCRETE)
(1)	(2)	(3) (4)	(5)	(6)	(9a)	(9b)	(9c)	(9d)	(9e)	(9f)	(9g)	(9h)	(9i)	(9j) (10)				
B	GS	ZB-FF-8-D	26±6	-	150	50	1850	500	800	N/A	N/A	N/A	N/A	N/A	10	80	41.25	DRY AREA PLACEMENT ZERO BLEED FLOWABLE FILL w/No. 8 STONE (7) (8)

For the Structural Flowable Fill Zero Mix: the notes of Attachment 5.5, page 4 of 4 apply with exception as listed below.

(4) N/A
(5) Flow/Slump Working Range. Flow/Slump is measured according to ASTM C1611/C1611M
(9k) HRWR is W. R. Grace Advacast 575.
(9l) VMA is W. R. Grace EXP-958

AFTER

THIS DCF

SRN 19-0082.0. "Test Report—CLSM Proposed TCG Hydraulic Conductivity Test (Transmittal letter from Jianren Wang to William Joyce with attached test results)." Atlanta, Georgia: Wood Environment & Infrastructure Solutions, Inc. May 7, 2020. [ADAMS Accession No. ML23087A006]

This is a test report transmittal letter conveying hydraulic conductivity (K_{sat}) test results for three samples of a proposed Zero-Bleed, Controlled Low-Strength Material (ZB-CLSM), slag-free tank closure grout (TCG) in its Attachment 1 to Savannah River Nuclear Solutions (SRNS).
The ZB-CLSM grout samples were prepared from grout mix ZB-FF-8-D and had aged 90 days (SREL Doc. R-21-0003) prior to testing. The saturated hydraulic conductivity tests were conducted in accordance with ASTM D 5084-16a, Method F (Constant Volume Falling Head) using a flexible wall permeameter by Wood Environment & Infrastructure Solutions, Inc. under SRNS Subcontract No. 0000441257. Results are summarized in the following table.

Sample No.	Mean Hydraulic Conductivity at 20 °C [68 °F] and 90 days (cm/s)
20014-1A	2.0×10^{-8}
20014-1B	1.1×10^{-8}
20014-1C	3.1×10^{-8}
Mean	**2.1×10^{-8}**

SRR-CWDA-2020-00045. Flach, G. “Characterization and Assessment of CLSM Grouts for Potential Use in Waste Tank Operational Closures.” Revision 0. Aiken, South Carolina: Savannah River Remediation. June 2020. [ADAMS Accession No. ML22094A047]

This report evaluates two CLSM grout mix candidates (EXE-X-P-0-X and ZB-FF-8-D) for potential use as bulk tank-fill grout when physical stabilization is necessary but radiochemical stabilization is not. Candidate tank-fill grouts are flowable, self-leveling and self-consolidating without vibration. Requirements for grout set time under 24 hrs and zero bleed after 24 hrs were proposed to enable daily placement of fresh grout above hardened, hydrating grout. Neither a grout recommendation nor a grout selection decision for tank closure were within the scope of this study.

System One, Inc. mixed EXE-X-P-0-X and ZB-FF-8-D CLSM grouts and performed fresh grout property measurements (i.e., slump flow, bleed and set time), compressive strength tests, and shrinkage tests. Wood Environment & Infrastructure Solutions, Inc. conducted saturated hydraulic conductivity (K_{sat}) tests on the grout specimens after 90 days had elapsed (see SRN 19-0082.0). The purposes of this characterization and assessment study were to (i) identify grout attributes affecting performance as a liquid waste tank bulk fill material (captured in their Table 3); (ii) define performance metrics, requirements, and goals (captured in their Table 3); (iii) assemble existing material property characterization data on LP#8-16 reducing tank grout mix (used to fill Tanks 5F, 6F, 12H, 16H, 18F, and 19F) and the EXE-X-P-0-X and ZB-FF-8-D CLSM grout mixes; (iv) identify key data gaps and acquire new CLSM material property data; (v) assess pros and cons of LP#8-16 reducing tank grout and the EXE-X-P-0-X and ZB-FF-8-D CLSM grout mixes on an attribute-by-attribute basis (Section 4 and Tables 11 and 12 of the report), and (vi) recommend next steps for selection of a bulk fill tank grout for future waste tank operational closures (Section 5 of the report) when radiochemical stabilization is unnecessary based on tank inventory.

Potential use of the inexpensive EXE-X-P-0-X CLSM grout mix likely will be abandoned for tank closure grout based on its characterization data. The mix produces an excessive amount of bleedwater (Table 8 of report; see also SREL Doc. R-21-0001 Figure 2 and SRR-CWDA-2015-00109). Additionally, its K_{sat} was only slightly lower than that of backfill soil and it may not have been able to maintain a *pH* high enough for corrosion protection. Finally, its compressive strength at 90 days was insufficient to meet the NRC-recommended 3,450 kPa [500 psi] threshold.

In contrast, Zero-Bleed CLSM mix ZB-FF-8-D was designed to produce no bleedwater 24 hrs after being placed. The ZB-FF-8-D grout mix formula is similar to the grout mix placed into Tanks 17F and 20F, and this grout has been used extensively at SRS for more than a decade, including during decommissioning of P- and R-Reactor complexes (SRNL-STI-2019-00009; Langton et al. 2010; Langton et al. 2011). In fact, the ZB-FF-8-D grout mix formed the basis for later development of LP#8-16 reducing tank grout. The compressive strength of mix ZB-FF-8-D at 90 days exceeded both the NRC’s 410 kPa [60 psi] requirement and the NRC’s 3,450 kPa [500 psi] recommendation. Mix ZB-FF-8-D exhibited near-zero net bleed at 24 hrs (Table 9 of report) and no shrinkage. Its K_{sat} was roughly three orders of magnitude lower than that of backfill soil, and its *pH* was greater than 10, as needed for corrosion protection. In comparison to LP#8-16 reducing tank grout, however, LP#8-16 has higher compressive strength, lower K_{sat}, and higher *pH* than ZB-FF-8-D. There is also virtually no price difference between these two mix options.

The report concluded by recommending that the effective diffusion coefficient and water-retention properties of mix ZB-FF-8-D be characterized, which were subsequently documented in SREL Doc. R-21-0003 with a *w:cm* ratio of 0.595 instead of 0.641.

SREL Doc. R-21-0001. Seaman et al. “Aqueous and Solid Phase Characterization of Potential Tank Fill Materials.” Aiken, South Carolina: Savannah River Ecology Laboratory. August 20, 2020. [ADAMS Accession No. ML20303A339]

To address uncertainty in realistically achievable oxidation–reduction potential (E_h) ranges for bulk fill tank grout alternatives, Savannah River Ecology Laboratory (SREL) characterized the aqueous chemistry of three candidate tank-fill grouts via a series of batch and column tests under a realistic range of atmospheric conditions: (i) LP#8-16 reducing tank grout referred to herein as Tank Closure Grout (TCG; 18% ordinary Portland cement; 30% ground granulated blast furnace slag; 52% fly ash), which has been used to fill Tanks 5F, 6F, 12H, 16H, 18F, and 19F; (ii) slag-free LP#8-16 (slag replaced by fly ash, similar to but not the same as Zero-Bleed CLSM mix ZB-FF-8-D), referred to herein as Tank Closure Grout with No Blast Furnace Slag (TCG-NBFS; 18% ordinary Portland cement and 82% fly ash), and (iii) EXE-X-P-0-X (7.7% ordinary Portland cement and 92.3% fly ash), referred to as CLSM or Common CLSM but not to be confused with TCG-NBFS nor with Zero-Bleed CLSM mix ZB-FF-8-D.

The TCG (also called TFG for Tank Fill Grout in the previous table) and TCG-NBFS/TFG-NBFS grout mixes had tap-water-to-cementitious material ratios (*w:cm*) of 0.579, whereas grout mix EXE-X-P-0-X (called common CLSM in the previous table) had *w:cm* = 0.847.

These three representative grout pastes (no aggregate) hydrated and aged for 90 days, then were size-reduced or granulated to ≤2 mm for use in batch tests or mixed with clean quartz Ottawa sand consistent with the amount called for in the grout formulas to homogenize flow in column tests. Sand mixed with the particulate grout was deemed necessary for the column tests to maintain constant flow while reproducing the formulated proportions of cementitious materials vs. sand in monolithic grout recipes. In column experiments, the particulate grout plus sand were leached under saturated conditions with pore-water simulant either oxidized or else N_2-purged. Sand was not used in the grout formulation for batch tests because the quartz peak associated with sand would overwhelm XRF results (i.e., quartz peak interference; see ML21026A012). In batch experiments, the grout particulate matter was equilibrated with a pore-water simulant for 150+ days; *pH* and E_h were monitored weekly and small aliquots of leachate were sampled weekly and analyzed for major elements by ICP-MS.

LP#8-16 reducing tank grout/TCG maintained the highest *pH*, necessary for corrosion protection, with TCG-NBFS having the next-highest *pH*. Lowest E_h values were attained for all samples equilibrated in an anaerobic Coy Chamber, and the next-lowest values were attained for samples equilibrated with a purged nitrogen atmosphere in a glove box; highest values were associated with batch samples open to the lab atmosphere. For more detail, see SRR-CWDA-2020-00061, Table 1.

Original dry feed cementitious materials, the three non-leached candidate reference tank grouts, and leached grout samples also underwent solid-phase characterization by X-ray fluorescence (XRF) spectroscopy (as borate fused bead samples) and X-ray diffraction (XRD) spectroscopy. Inert quartz, mullite, hematite and magnetite crystalline phases in semi-amorphous fly ash were detected in both non-leached and leached samples. Non-leached samples contained strätlingite, calcite, ettringite, and varied alumina, ferric oxide, and monosulfate (AFm). Leached samples did not contain ettringite, and AFm either disappeared or else decreased.

Strätlingite persisted in most of the leached samples but was barely detected in any grout samples exposed to a reducing environment and was also barely detected in LP#8-16 reducing tank grout/TCG samples subjected to any environment. Calcite persisted in all samples and especially those subjected to an oxygenated atmosphere due to carbonation in the CO_2-containing oxic environment. Hydrotalcite and possibly kuzelite or monosulfoaluminate were only observed in LP#8-16 reducing tank grout/TCG samples; both minerals persisted in all leached LP#8-16 reducing tank grout/TCG samples regardless of atmosphere. Hydrotalcite was expected to be present because of the magnesia (MgO) content of the slag cement (approximately 6wt% measured via XRF). Monosulfoaluminate is produced via reaction between tricalcium aluminate (a primary cement phase) and ettringite (a cement hydration product).

SRR-CWDA-2020-00061. Flach, G.P. "Memorandum: Application of Characterization of the Aqueous and Solid Phase Chemistry of Closure Grouts." Revision 0. Aiken, South Carolina: Savannah River Remediation. August 25, 2020. [ADAMS Accession No. ML20303A345]

To address uncertainty in realistically achievable E_h ranges for tank grout, SREL characterized the aqueous chemistry of three candidate tank-fill grouts via a series of batch and column studies under a range of atmospheric conditions (SREL Doc. R-21-0001): (i) LP#8-16 reducing tank grout referred to herein as Tank Closure Grout (TCG; 18% ordinary Portland cement; 30% ground granulated blast furnace slag; 52% fly ash); (ii) slag-free LP#8-16 (slag replaced by fly ash similar to mix ZB-FF-8-D, referred to herein as Tank Closure Grout with No Blast Furnace Slag (TCG-NBFS; 18% ordinary Portland cement and 82% fly ash), and (iii) EXE-X-P-0-X (7.7% ordinary Portland cement and 92.3% fly ash), referred to as CLSM or Common CLSM (not to be confused with Zero-Bleed CLSM mix ZB-FF-8-D). Test conditions were (i) open, oxidizing atmosphere, (ii) N_2-purged atmosphere, (iii) closed, reducing atmosphere. Batch equilibration and column test results are summarized in Table 1 of the report, reproduced in this summary.

Original dry feed cementitious materials, the three candidate reference tank grouts (i.e., non-leached), and leached grout samples subjected to various batch equilibration conditions also underwent solid-phase characterization by XRF (as borate fused bead samples) and XRD analyses (SREL Doc. R-21-0001). Resulting empirical grout mineralogy data may be used to test reactivity assumptions for and update mineralogy assumptions in the waste release model. The identified mineral phases are summarized in Tables 2 and 3 of the report, reproduced in this summary.

Updates to the tank farm waste release model are anticipated to use these new data to address the (i) impact of infiltrating groundwater on grout pore-water chemistry as a function of time; (ii) anticipated mineral states; and (iii) solubility-controlling mineral phases selected per element.

The report concludes that the open-atmosphere and nitrogen-purge leaching conditions comprise reasonable upper and lower E_h endpoints for realistic field conditions inside waste storage tanks, and that this range is smaller than previously considered in SRNL-STI-2012-00404, which could affect radionuclide solubilities used in future PA modeling. Additionally, the report also concluded that E_h > 0.45 V is not realistic, but that a limit of ~0.35 V was supported by observations, suggesting that Pu solubility should be limited in Region II conditions. Further, the report concluded that E_h less than −0.29 V cannot be achieved with LP#8-16 reducing tank grout/TCG; in this study, the lowest E_h achieved for TCG under nitrogen-atmosphere conditions was −0.12 V, similar to a previously observed low E_h of −0.07 V (SRR-CWDA-2016-00086). There is little solubility control of Tc at E_h greater than −0.1 V in Reduced Region II conditions. Finally, the report concludes that under realistic,

Table 1: Summary of Batch Equilibration Results (SREL Doc.: R-21-0001) Compared to Geochemical Modeling Values for Reducing Grouts (SRNL-STI-2012-00404; SRR-CWDA-2016-00086)

	pH	Eh (volts)	Ca^{2+} (molar)	Na^{+} (molar)	Mg^{2+} (molar)	K^{+} (molar)
Leaching solution prescribed in SRNL-STI-2012-00404						
	4.68		2.1E-06	8.7E-06	1.3E-06	
Chemical Conditions of Reducing Grout Pore Water (SRNL-STI-2012-00404; SRR-CWDA-2016-00086)						
Red. Region II	11.1	-0.47	4.0E-03	1.0E-03		
Ox. Region II	11.1	0.56	4.0E-03	1.0E-03		
Ox. Region III	9.2	0.68	6.6E-05	1.0E-03		
Test Conditions	Current Study					
Batch Test - Open Atmosphere*	pH Range	Eh Range (Volts)	Ca^{2+} (molar)	Na^{+} (molar)	Mg^{2+} (molar)	K^{+} (molar)
TCG	11.1-12.6	0.12-0.26	2.0E-04	2.3E-04	3.6E-06	7.1E-04
TCG-NBFS	10.1-12.4	0.16-0.28	3.1E-04	2.2E-04	6.0E-06	8.2E-04
CLSM	9.2-11.9	0.20-0.35	3.5E-04	1.0E-04	1.1E-05	2.3E-04
Batch Test - N_2 Purged Atmosphere						
TCG	12.1-12.7	(-0.12)-0.18	ND	ND	ND	ND
TCG-NBFS	11.5-12.2	0.003-0.22	ND	ND	ND	ND
CLSM	10.8-11.8	0.02-0.27	ND	ND	ND	ND
Batch Test Coy Chamber - Reducing Atmosphere*						
TCG	11.6-12.8	(-0.42)-0.16	2.8E-04	1.3E-04	1.6E-06	4.3E-04
TCG-NBFS	11.0-12.4	(-0.36)-0.23	5.8E-05	2.3E-04	5.3E-07	1.2E-03
CLSM	9.22-12.1	(-0.45)-0.30	3.1E-04	1.1E-04	4.5E-06	3.4E-04
Column Test - Open Atmosphere**						
TCG	11.3-12.5	0.01-0.26	3.4E-04	6.0E-05	4.5E-07	7.3E-05
TCG-NBFS	10.9-12.3	0.13-0.35	7.7E-04	7.3E-05	1.8E-06	1.7E-04
CLSM	10.7-11.9	0.17-0.35	7.5E-04	5.6E-05	3.4E-06	8.8E-05
Column Test - N_2 Purged Atmosphere**						
TCG	11.3-12.5	(-0.03)-0.17	9.1E-04	6.5E-05	7.0E-07	1.1E-04
TCG-NBFS	11.0-12.1	0.10-0.25	8.0E-04	5.8E-05	1.4E-06	1.3E-04
CLSM	10.6-12.0	0.13-0.31	6.1E-04	4.9E-05	2.1E-06	1.0E-04

*Cation data for batch tests reflect the final solution after the "enhanced leaching" treatment.
**Cation data for column experiments reflect the final effluent composition.

open-atmosphere conditions, LP#8-16 reducing tank grout/TCG E_h observed was ≤0.26 V at ≤150 days, consistent with similar values previously assumed for Region II and Region III (SRNL-STI-2012-00404). Longer oxygen exposure may result in higher E_h for LP#8-16 reducing tank grout. For non-slag-bearing candidate tank grouts TCG-NBFS and EXE-X-P-0-X, however, E_h was observed ≤0.35 V. While E_h > 0.24 V does not increase Np solubility in Region II, E_h = 0.35 V does increase Np solubility in Region III. Therefore, Np solubility for Region III will likely be increased in PA modeling for any waste storage tanks filled with a non-slag-bearing, non-reducing grout. The report recommended a general reanalysis of realistic E_h assumptions be conducted, especially for modeling Tc and Np solubilities.

Table 2: Summary of Mineral Phases Identified Through XRD.

PHASE	SAMPLES OBSERVED IN			CONFIDENCE LEVEL
	CLSM	TCG-NBFS	TCG	
Strätlingite $Ca_2Al_2SiO_7.8H_2O$	• CLSM-REF • CLSM-OPEN • CLSM-CLOSED • CLSM-N_2	• TCG-NBFS-REF • TCG-NBFS-OPEN • TCG-NBFS-N_2	• TCG-REF • TCG-OPEN • TCG-CLOSED • TCG-N_2	HIGH
Ettringite $Ca_6Al_2(SO_4)_3(OH)_{12}(H_2O)_{26}$	• CLSM-REF	• TCG-NBFS-REF	• TCG-REF	HIGH
Kuzelite $Ca_2Al(SO_4)_{0.5}(OH)_6(H_2O)_3$	• Not Observed	• Not Observed	• TCG-REF • TCG-OPEN • TCG-CLOSED • TCG-N_2	MEDIUM
Calcium Iron Oxide Sulfite Hydrate $Ca_4Fe_2O_6(SO_3).12H_2O$	• Not Observed	• Not Observed	• TCG-REF • TCG-CLOSED • TCG-N_2	LOW
Calcium Aluminum Silicate Hydrate $CaAl_2Si_7O_{18}.1.7H_2O$	• Not Observed	• TCG-NBFS-REF	• Not Observed	LOW
Calcium Aluminum Oxide Carbonate Sulfate Hydroxide Hydrate $3CaO.Al_2O_3.0.17CaSO_4.0.5Ca(OH)_2.0.33CaCO_3.xH_2O$	• CLSM-REF	• Not Observed	• TCG-REF • TCG-OPEN	LOW
Calcium Aluminum Carbonate Hydroxide Hydrate (Hemicarboaluminate) $Ca_2Al(CO_3)_{0.25}(OH)_{6.5}(H_2O)_2$	• CLSM-REF	• TCG-NBFS-REF	• TCG-REF	MEDIUM
Calcium Aluminum Iron Oxide Carbonate Hydroxide Hydrate $Ca_8Al_2Fe_2O_{12}CO_3(OH)_2.22H_2O$	• CLSM-REF	• TCG-NBFS-REF • TCG-NBFS-CLOSED • TCG-NBFS-N_2	• TCG-OPEN • TCG-CLOSED • TCG-N_2	LOW
Hydrotalcite $Mg_{0.67}Al_{0.33}(CO_3)_{0.17}(OH)_2(H_2O)_{0.5}$	• Not Observed	• Not Observed	• TCG-REF • TCG-OPEN • TCG-CLOSED • TCG-N_2	MEDIUM
Calcium Aluminum Carbonate Hydroxide Hydrate (Monocarboaluminate) $Ca_4Al_2(CO_3)(OH)_{12}(H_2O)_5$	• CLSM-REF	• TCG-NBFS-REF • TCG-NBFS-CLOSED • TCG-NBFS- N_2	• Not Observed	MEDIUM
Mullite *General:* $3Al_2O_3.2SiO_2$ *Actual:* $Al_2(Al_{2.588}Si_{1.412})O_{9.706}$	• All Samples	• All Samples	• All Samples	HIGH
Portlandite $Ca(OH)_2$	• Not Observed	• Not Observed	• TCG-REF • TCG-OPEN • TCG-CLOSED • TCG-N_2	MEDIUM
Quartz SiO_2	• All Samples	• All Samples	• All Samples	HIGH
Calcite $CaCO_3$	• All Samples	• All Samples	• All Samples	HIGH
Hematite Fe_2O_3	• All Samples	• All Samples	• All Samples	HIGH
Silicon *Si*	• All Samples	• All Samples	• All Samples	HIGH
Calcium Silicate Hydrates *C-S-H*	• Possibly present in all samples but most predominant in TCG-REF			MEDIUM
Magnetite Fe_3O_4	• All Samples	• All Samples	• All Samples	HIGH

Table 3: Summary of Rietveld Quantification Results for the Three Pastes.

CLSM Sample	Phase (wt%)									
	Amorphous	*Mullite*	*Quartz*	*Hematite*	*Magnetite*	*Calcite*	*Strätlingite*	*Ettringite*	*Hemicarbo-aluminate*	*Monocarbo-aluminate*
REF (Non-Leached)	66.12	14.11	10.23	2.09	1.10	0.88	2.72	0.49	1.88	0.38
OPEN	65.55	14.75	10.95	2.12	1.48	3.01	2.14	-	-	-
CLOSED	68.79	14.75	11.19	2.12	1.64	1.51	Trace *	-	-	-
N_2	66.92	15.24	11.24	2.14	1.69	1.10	1.71	-	-	-

* Trace is indicated for strätlingite because the peak is barely above background and its inclusion (at such low concentrations) for Rietveld refinement resulted in pattern simulation anomalies; hence it was omitted during Rietveld quantification

TCG-NBFS Sample	Phase (wt%)									
	Amorphous	*Mullite*	*Quartz*	*Hematite*	*Magnetite*	*Calcite*	*Strätlingite*	*Ettringite*	*Hemicarbo-aluminate*	*Monocarbo-aluminate*
REF (Non-Leached)	66.97	11.69	8.64	1.79	0.99	2.63	1.85	1.41	2.61	1.43
OPEN	68.66	11.87	9.07	1.81	1.01	6.08	1.51	-	-	-
CLOSED	72.58	11.32	9.12	1.73	1.07	2.79	-	-	-	1.39
N_2	71.17	11.77	8.55	1.86	0.79	2.27	1.75	-	-	1.84

TCG Sample	Phase (wt%)											
	Amorphous	*Mullite*	*Quartz*	*Hematite*	*Magnetite*	*Calcite*	*Ettringite*	*Strätlingite*	*Hydrotalcite*	*Kuzelite*	*Portlandite*	*Hemicarbo-aluminate*
REF (Non-Leached)	78.40	6.06	5.44	1.22	0.14	1.14	0.91	Trace *	1.42	0.78	0.42	4.07
OPEN	77.85	6.55	5.64	1.30	0.22	5.37	-	Trace	2.67	0.41	-	-
CLOSED	78.92	5.48	5.28	1.29	0.15	3.38	-	Trace	3.07	1.75	0.08	-
N_2	79.66	6.64	5.96	1.44	0.24	1.30	-	Trace	2.78	1.77	0.20	-

* Trace is indicated for strätlingite because the peak is barely above background and its inclusion (at such low concentrations) for Rietveld refinement resulted in pattern simulation anomalies; hence it was omitted during Rietveld quantification.

SRR-CWDA-2020-00085. Flach, G. "Tank Grout Bulk Chemistry Experiments (Slide Presentation)." Revision 1. Aiken, South Carolina: Savannah River Remediation. December 2020.

Gregory Flach presented results of SREL research (i.e., SREL R-21-0001) to NRC staff at an onsite observation visit. He addressed the uncertainties that motivated SREL's grout bulk chemistry experiments, then summarized the grout paste samples prepared [i.e., Tank Fill Grout (TFG), Tank Fill Grout with No Blast Furnace Slag (TFG-NBFS), and Common CLSM (EXE-X-P-0-X)], atmospheric conditions applied, and batch, column, and XRD test methods applied by SREL. SREL results showed the E_h endpoints assumed in PA modeling were not achieved (both high and low E_h values). The impact of E_h on solubility of key radionuclides and thoughts

on future work were also discussed. Gregory Flach mentioned that updated geochemical modeling would be pursued to better understand radionuclide solubility.

Concluding preliminary thoughts were presented as:

- **PA validations:** Alkali metals leave quickly, predicted mineralogy generally consistent, *pH* prediction good, solubilities based on E_h lower than model prediction for oxidized conditions
- **Opportunities:** Add hemicarboaluminate to mineral set, consider partial hydration, update C-S-H solid solution model, better predict E_h, reconsider E_h range for solubility assignments
- ***E_h* challenges:**
    - E_h probes biased with respect to some redox couples.
    - Disequilibrium of experiments due to short timescale.
    - Modeling assumes equilibrium but there is inherent redox disequilibrium, even at long times.
    - Integrate experimental and modeling insights.

SREL Doc. R-21-0003 (also SRRA099188-000015). Seaman et al. "CLSM Characterization: Data Report." Aiken, South Carolina: Savannah River Ecology Laboratory. September 21, 2021. [ADAMS Accession No. ML21336A379]

This document provides grout characterization test results obtained by SREL for performance attributes of Zero-Bleed CLSM grout mix ZB-FF-8-D batched with a *w:cm* ratio of 0.595 instead of 0.641 (see its Table 1, reproduced next).

Table 1. CLSM (mix ZB-FF-8-D) as-designed versus as-batched mix proportions on February 4, 2020 (SRR-CWDA-2020-00045).

Ingredient	Mix Design	As-Batched	Units	Ratio
Cement	150	153.3	lbs/yd^3	1.022
Fly Ash	500	503.3	lbs/yd^3	1.007
Sand	1850	1960	lbs/yd^3	1.059
Aggregate	800	786.7	lbs/yd^3	0.983
Water	50	46.9*	gal/yd^3	0.937
	416.5	390.4	lbs/yd^3	
w/cm ratio	0.641	0.595	-	
Density	8.33	8.33	lbs/gal	

*batched + added water

SREL conducted K_{sat} tests in accordance with ASTM D 5084-16a, Method F (Constant Volume Falling Head) using a flexible wall permeameter and measured K_{sat} of four ZB-FF-8-D grout samples that had aged a minimum of 316 days and compared these results (mean $K_{sat} = 1.8 \times 10^{-8}$ cm/s) with those reported by Wood Environment & Infrastructure Solutions, Inc. (mean $K_{sat} = 2.1 \times 10^{-8}$ cm/s) for grout samples aged 90 days (see SRN 19-0082.0 and the following table).

Sample No.	Mean K_{sat} (cm/s) at >300 days
A	2.3×10^{-8}
B	0.4×10^{-8}
C	3.7×10^{-8}
D	0.8×10^{-8}
Mean	**1.8×10^{-8}**

SREL also estimated water retention or moisture characteristic of three of the four ZB-FF-8-D grout samples tested for K_{sat}. The air entry pressure of this grout exceeds 500 kPa [72.5 psi].

Finally, SREL estimates of apparent tritium diffusion coefficient for two ZB-FF-8-D grout samples were 1.0×10^{-8} $cm^2 \cdot s^{-1}$ and 3.6×10^{-8} $cm^2 \cdot s^{-1}$ using a modified sample immersion method (Park et al., 2014); these results were similar to values for nitrate. SREL was unable to calculate chloride diffusion coefficient, however, because the error bars were too large (see their Figure 6). Nevertheless, the general trend in chloride concentration was similar to tritium.

Performance Assessment Maintenance Plans

SRMC-CWDA-2023-00045. "Savannah River Site Liquid Waste Facilities Performance Assessment Maintenance Program, FY2023." Revision 0. Aiken, South Carolina: Savannah River Mission Completion. June 2023.

Plans to support the PA for the SRS Tank Farm Facilities is presented in this report.

Planned activities include:

1. Groundwater sampling until the waste tanks and ancillary equipment are removed from service as dictated by the final Record of Decision for the FTF and HTF Groundwater Operable Units according to the new sampling and analysis plans.
2. Any unreviewed waste management question process activities or UWMQE [to resolve questions or issues that arise that appear to be outside the bounds of the approved NDAA Section 3116 Basis Document, PA, composite analysis (CA), or special analysis (SA)]. No UWMQE were conducted in 2022 and none are identified at this time but for planning purposes four are assumed for each year over the next 5 years.
3. Annual update to the PA maintenance plan to confirm the adequacy of the current PA and SA.
4. General technical support on tank farm performance assessment issues including addressing any regulatory issues that arise and to support onsite observations and technical reviews. These activities include research activity support with outside agencies as well as onsite research. These activities support SC DHEC, SRS CAB, LFRG, and NAS and other regulatory and stakeholder bodies.
5. Develop and maintain PA models in archive and revision control including improvements in storage and maintenance of modeling files such as GoldSim and PORFLOW.
6. PA revisions including updates to the HTF and FTF PAs expected to be completed in FY2024[7]. The revisions will consider information from NRC's technical evaluation reports, technical review reports (TRRs), and combined FTF and HTF monitoring plan.
7. Tank Farm Special Analyses to evaluate the significance of new information or new analytical methods on the results and associated conclusions of a PA. For example,

[7] Note the PA Maintenance Plan has date of FY2023, but as of the date of this note to file, the PA has not yet been submitted to the NRC for review and current estimates are the end of CY2023.

when tanks are cleaned and closed, and a final inventory developed, an SA is performed to revise PA dose estimates.

No waste-release testing, residual waste characterization, controlled low-strength material (CLSM) grout testing, or closure cap design evaluations were performed in FY2022 and none were planned for FY2023.

Appendix C lists monitoring items taken from recommendations or action items from the FTF and HTF TERs, the FTF/HTF combined monitoring plan, and various TRRs written since NRC monitoring began.

Comments:

1. Several documents were developed to support the PA and are listed in the PA Maintenance Plan. NRC requested the following references some of which are evaluated in this note to file:
    a. SRR-CWDA-2020-00074, “Features, Events, and Processes for the F-Area and H-Area Tank Farm Performance Assessments,” March 2021.
    b. SRR-CWDA-2019-00104, “Strategy for Updating the SRS Tank Farm Performance Assessments,” December 2019.
    c. SRMC-CWDA-2022-00036, Rev. 1, “Recommended Infiltration Rate for HTF Barrier Analysis that Assumes Initially Failed Saturated Hydraulic Conductivities,” August 2022.
    d. SRR-CWDA-2013-00058, Rev. 3, “Dose Calculation Methodology for Liquid Waste Performance Assessments at the Savannah River Site,” January 2022.
    e. SRMC-CWDA-2023-00009, “Aquifer Transport Model Abstraction for 2023 H -Tank Farm (HTF) Performance Assessment (PA), January 2023.
    f. SRR-CWDA-2021-0004, “Conceptual Model Development for the H-Area Tank Farm Facility Performance Assessment,” March 2021.
2. The last three TRRs issues by NRC in 2020 and 2021 were not listed at the end of the Appendix C follow-up monitoring items. These reports are:

NRC Technical Review Report (Tank 12H Grouting)	11/18/2020	ML20296A550
NRC Technical Review Report (Environmental Monitoring)	05/14/2021	ML21119A312
NRC Technical Review Report (Type I and II Tank SA)	09/01/2021	ML21231A202

SRMC-CWDA-2022-00006. “Savannah River Site Liquid Waste Facilities Performance Assessment Maintenance Program, FY 2022.” Revision 0. Aiken, South Carolina: Savannah River Mission Completion. May 2022.

The 2022 PA maintenance plan listed several documents in the (i) waste release, (ii) CLSM grout testing, and (iii) closure cap technical areas that had been completed. No additional work was planned for FY2022 through FY2026, although 50K was allotted for engineered cover work (unclear how this money would be used). Similar activities to what was listed in the 2023 PA maintenance plan were also listed including (i) UWMQE allotment, (ii) PA maintenance program, (iii) general technical support for tank farm PAs, (iv) development and maintenance of PA model archive and revision control, and (v) updates to the HTF and FTF PA.

Comments:

1. Several documents developed to support the PA are listed in the 2022 PA Maintenance Plan. NRC requested and received the following references that were not listed in the 2023 PA Maintenance Plan (some of these references are reviewed in this note to file):
    a. SRNL-STI-2021-00017, "Geochemical Data Package for Performance Assessment Calculations Related to the Savannah River Site," 2021.
    b. SRR-CWDA-2021-00025, "Tank Farm Closure Inventory for use in Performance Assessment Modeling," March 2021.
    c. SRR-CWDA-2021-00045, Air Pathway Release Model for the F-Area and H-Area Tank Farm Facility Performance Assessments," May 2021.
    d. SRR-CWDA-2021-00078, "Saturated Hydraulic Conductivities for F-Area and H-Area Tank Farm Cementitious Materials," September 2021.
    e. SRR-CWDA-2013-00058, Rev. 3, "Dose Calculation Methodology for Liquid Waste Performance Assessments at the Savannah River Site," January 2022.

Tank Inspection Reports

SRMC-STI-2023-00011. "Annual Radioactive Waste Tank Inspection Program—2022." Revision 0. Aiken, South Carolina: Savannah River Mission Completion. June 2023.

In 2022, DOE performed inspections of 43 operational HLW tanks[8] through all accessible annulus risers and inspection ports that have not been closed for Type I, II, and III tanks; and at least one inspection was made on the interior of four Type IV tanks. Evidence of rainwater in-leakage into the annuli of some tanks was observed, including surface stains, occasional calciferous deposits, changed configuration of salt deposits and mild surface corrosion. The 2022 inspection program confirmed the structural integrity and waste confinement capability of all 43 waste tanks. Additionally, above-ground transfer lines, transfer jet steam and air isolation valves, diversion box ventilation systems/passive vents, waste tank chromate water header and coil isolation valves, and other ancillary equipment were inspected. No material degradation of the ancillary equipment that would prevent its performing was noted. Ultrasonic testing was performed on Tanks 41, 43, 49 and 50 as scheduled.

No significant changes in conditions were noted between the 2021 and 2022 inspections except for Tank 10H. The 2022 report noted 17 new cracks in the Tank 10H primary tank wall between 1.83 and 3.28 m [72 and 129 in] above the tank bottom and one site at an unknown elevation above the tank bottom.

SRMC-STI-2022-00154. "Annual Radioactive Waste Tank Inspection Program—2021." Revision 0. Aiken, South Carolina: Savannah River Mission Completion. June 2022.

In 2021, DOE performed inspections of 43 operational HLW tanks[9] through all accessible annulus risers and inspection ports that have not been closed for Type I, II, and III tanks; and at least one inspection was made on the interior of four Type IV tanks. Evidence of rainwater in-leakage into the annuli of some tanks was observed including surface stains, occasional calciferous deposits, changed configuration of salt deposits and mild surface corrosion. The 2021 inspection program confirmed the structural integrity and waste confinement capability of all 43 waste tanks. Additionally, process vessel ventilation system, diesel generator HDB-8,

[8] A total of 8 of 51 HLW tanks have been operationally closed: Tanks 5F, 6F, and 17F–20F at FTF; and 12H and 16H at HTF.
[9] A total of 8 of 51 HLW tanks have been operationally closed: Tanks 5F, 6F, and 17F–20F at FTF; and 12H and 16H at HTF.

evaporator primary ventilation system, and other ancillary equipment were inspected. No material degradation of the ancillary equipment that would prevent its performing was noted. Ultrasonic testing was performed on Tanks 47, 48, and 51. Inspections performed in Tanks 25 and 41 were per the Corrosion Control Program. The inspections revealed no reportable thinning, pitting, stress corrosion cracking, or evidence of service-induced thinning of the primary tank wall, or the secondary linear wall and floor.

No significant changes in conditions were noted between the 2020 and 2021 inspections except for Tank 10H. The 2021 report noted 2 new cracks in the Tank 10H primary tank wall at 2.79 and 3.28 m [110 and 129 in] above the tank bottom.

Appendix B
Follow-up Questions:

Waste Release

1. Many dissolved species were eliminated to simplify *The Geochemist's Workbench*® models. Could DOE clarify how it ensured that these omissions would not affect calculated solubilities? For instance, Al and K can affect silicate mineral solubilities, which can affect dissolved silica and, therefore, uranophane solubility.
2. Could DOE clarify if saturation indices for other solids for a given radioelement were checked for supersaturation? Did DOE have to suppress any phases and, if so, were those suppressions justified?
3. DOE should confirm that of the more important radioelements, only U solubilities were updated based on new experimental data.
4. The results present modeled solubilities. Will DOE consider any other data from waste-release experiments or other sources for the updated PA? For instance, Pu solubilities changed little from the 2012 report (i.e., SRNL-STI-2012-00404). All values are approximately 1×10^{-11} M except at $pH < 6$, where the Pu solubility does not exceed 1×10^{-8} M.

Alternative Grout Formulations

1. Would DOE confirm that it has abandoned consideration of use of the Common CLSM grout mix EXE-X-P-0-X as a potential alternative tank fill grout based on its characterization data? This grout mix produces bleedwater and its K_{sat} is only slightly lower than that of backfill soil. It may not be able to maintain a pH high enough for corrosion protection, and its compressive strength at 90 days does not meet the NRC recommended 3,450 kPa [500 psi] threshold.
2. Slag-free "LP#8-16 tank closure grout" (TCG-NBFS or TFG-NBFS with additional fly ash replacing slag) is very similar to but not the same as zero-bleed CLSM mix ZB-FF-8-D. Would DOE clarify which of these two slag-free grouts it tends to prefer as a potential alternative to reducing LP#8-16 tank grout when radiochemical stabilization is unnecessary?
3. Would DOE clarify if ZB-FF-8-D is the slag-free grout placed into Tanks 17F and 20F?

Note to File Related to SRS Tank Farm 2022 and 2023 Monitoring Activities and Preliminary Review of HTF PA Documents DATE January 16, 2024

DISTRIBUTION:
GAlexander, NMSS/DUWP/RTAB
GNelson, NMSS/DUWP/LLWPB

ADAMS Accession No.: ML23361A032; ML23361A032 *** via email**

OFFICE	NMSS/DUWP /RTAB	NMSS/DUWP /LLWPB	NMSS/DUWP/RTAB	NMSS/DUWP/RTAB*
NAME	CBarr *CB*	GNelson *GN*	GAlexander *GA*	CMcKenney *CM*
DATE	Dec 27, 2023	Jan 4, 2024	Jan 9, 2024	Jan 12, 2024
OFFICE	NMSS/DUWP /RTAB			
NAME	CBarr *CB*			
DATE	Jan 16, 2024			

OFFICIAL RECORD COPY